CHALMERS

Design and Evaluation of Rear Axle Side Slip Stability Control for Passenger Cars

- Simulations and Experimental Verification of Interventions in Oversteer Situations

JOHAN BILLMARK

JONAS ÖSTH

Department of Applied Mechanics
Division of Vehicle Safety
CHALMERS UNIVERSITY OF TECHNOLOGY
Göteborg, Sweden 2007

Master's Thesis 2007:68

MASTER'S THESIS 2007:68

Design and Evaluation of Rear Axle Side Slip Stability Control for Passenger Cars

- Simulations and Experimental Verification of Interventions in Oversteer Situations

Master's Thesis in Automotive Engineering

JOHAN BILLMARK

JONAS ÖSTH

Department of Applied Mechanics
Division of Vehicle Safety
CHALMERS UNIVERSITY OF TECHNOLOGY
Göteborg, Sweden 2007

Design and Evaluation of Rear Axle Side Slip Stability Control for Passenger Cars
- Simulations and Experimental Verification of Interventions in Oversteer Situations
Master's Thesis in Automotive Engineering
JOHAN BILLMARK
JONAS ÖSTH

Master's Thesis 2007:68
ISSN 1652-8557
Department of Applied Mechanics
Division of Vehicle Safety
Chalmers University of Technology
SE-412 96 Göteborg
Sweden
Telephone: + 46 (0)31-772 1000

The work was performed at:
Volvo Car Corporation
Active Safety Functions, Dept. 96260
SE-405 31 Göteborg
Sweden
Supervisor: Bengt Jacobson

Chalmers Reproservice
Göteborg, Sweden 2007

Design and Evaluation of Rear Axle Side Slip Stability Control for Passenger Cars
- Simulations and Experimental Verification of Interventions in Oversteer Situations
Master's Thesis in Automotive Engineering

JOHAN BILLMARK
JONAS ÖSTH
Department of Applied Mechanics
Division of Vehicle Safety
Chalmers University of Technology

ABSTRACT

Vehicle stability control has had a remarkable effect on the active safety of passenger cars. Therefore further development of vehicle stability control systems is an ongoing activity in the automotive industry. The objective of this project was to develop a rear axle side slip angle controller to improve the stability control for passenger cars in oversteer situations. In these situations, the vehicle has a significant lateral velocity and can even start skidding sideways. This is a potentially dangerous condition because the vehicle is then also insensitive to steering wheel inputs from the driver. Interventions from the stability control system can prevent this condition and increase the active safety of passenger cars.

The developed controller is implemented in a simulation environment consisting of the vehicle dynamics simulation tool Vedyna available in Matlab/Simulink. To enable evaluation in vehicle tests the controller was developed as an extension to existing production like stability control functions.

For the evaluation in both simulations and vehicle tests two relevant test cases were chosen. The first test case was the J-turn maneuver, resembling a highway exit where the vehicle can experience oversteer as the result of a load transfer when decelerating. The second test case was an evasive maneuver in the form of a double lane change. The latter test case is used to verify that the vehicle maneuverability was not impaired by the developed controller.

Using rapid control prototyping tools the tests were also carried out in a vehicle on the test track to verify the previous results from the simulations. The results from simulations and experiments show that adding rear axle side slip angle control to regular stability control functions can improve the stability control in oversteer situations. The developed controller helps the driver to maintain control of the vehicle even if the driver reacts late in a maneuver like the J-turn. Furthermore, it was shown that the performance in evasive maneuvers can be enhanced rather than impaired by the developed controller. For the double lane change maneuver studied the entrance speed was increased by up to 2 km/h.

Lastly, it should be noted that the developed function is depending on a reliable estimation of the rear axle side slip angle, why further work is needed before the functionality can be industrialized.

Key words: active safety, electronic stability control, rear axle side slip angle control

Contents

Preface

This Master's Thesis was carried out at the Active Safety Functions group at Volvo Car Corporation and at the Department of Applied Mechanics at Chalmers University of Technology in Göteborg. The work was carried out from June to November 2007.

We would like to thank our supervisor at Volvo Cars, Dr. Bengt Jacobson, for making it possible for us to do our thesis in the interesting field of active safety and for his continuous support. We would also like to thank our supervisor at Chalmers University of Technology, Dr. Mathias Lidberg, for his input and feedback on the writing of the thesis.

Lastly we would like to thank everyone else at Volvo Cars that have supported us in our work: Jonas Adolfsson, Per Olsson and Anders Ödblom for their assistance with the vehicle dynamics simulations; Björn Eriksson, Andreas Bohlin and Mikael Riikonen for their help with planning and performing the vehicle tests; and Mats Jonasson for interesting discussions on vehicle dynamics.

Göteborg, November 16, 2007

JOHAN BILLMARK
JONAS ÖSTH

Notations

Upper-case roman letters

A_{pad}	Brake pad area	[m^2]
C_s	Longitudinal tire stiffness	[N]
C_α	Cornering tire stiffness	[N/rad]
F_i	Force	[N]
I_z	Yaw moment of inertia	[kgm^2]
L	Vehicle wheel base	[m]
K_p	Proportional controller gain	[Nm/rad]
K_{us}	Understeer coefficient	[-]
P_{req}	Brake pressure request	[bar]
R_w	Wheel radius	[m]
R_{disc}	Brake disc effective radius	[m]
$T_{z,req}$	Yaw moment request	[Nm]
V	Velocity	[m/s]
W	Weight	[N]
X	Earth fixed longitudinal axis	[m]
Y	Earth fixed lateral axis	[m]
Z	Earth fixed vertical axis	[m]

Lower-case roman letters

a_y	Lateral acceleration	[m/s^2]
e	Rear axle side slip control error	[rad]
g	Gravitational acceleration	[m/s^2]
l_1	Front axle distance to center of gravity	[m]
l_2	Rear axle distance to center of gravity	[m]
m	Vehicle mass	[kg]
s_{xi}	Longitudinal tire slip	[-]
w	Vehicle track width	[m]
x	Vehicle fixed longitudinal axis	[m]
y	Vehicle fixed lateral axis	[m]
z	Vehicle fixed vertical axis	[m]
z_i	Tire vertical displacement	[m]

Greek letters

α_i	Tire slip angle	[rad]
β	Vehicle side slip angle	[rad]
β_r	Rear axle side slip angle	[rad]
$\beta_{r,ref}$	Rear axle side slip reference angle	[rad]
δ_i	Wheel steer angle	[rad]
θ	Vehicle pitch angle	[rad]
μ	Friction coefficient	[-]
φ	Vehicle roll angle	[rad]
ψ	Vehicle yaw angle	[rad]
ω_i	Wheel rotational speed	[rad/s]

Acronyms

ABS	Anti-lock Braking System
AFS	Active Front Steering
BCM	Brake Control Module
CAN	Controller Area Network
CoG	Center of Gravity
DAS	Data Acquisition System
DOF	Degree(-s) of Freedom
ECU	Electronic Control Unit
ESC	Electronic Stability Control
FL	Front Left
FR	Front Right
NHTSA	National Highway Traffic Safety Administration
RL	Rear Left
RR	Rear Right
RSC	Roll Stability Control
SSA	Side Slip Angle
SSRA	Side Slip angle at the Rear Axle
SUV	Sports Utility Vehicle
SWA	Steering Wheel Angle
TCS	Traction Control System
VCC	Volvo Car Corporation

1 Introduction

Annually over 1.8 million people are injured and 43.000 fatalities are reported due to traffic accidents within the European Union, causing an estimated cost of 160 billion euros (European Road Safety Observatory, 2006a). Due to the effort of both the governments of Europe and car manufacturers like Volvo Cars, who put safety as their top priority, the fatality numbers have been decreasing over the last 20 years. However, to meet the goal stated by the European Commission, that by the year 2010 the annual fatality number should be decreased to 25.000, even further advances in vehicle safety needs to be made.

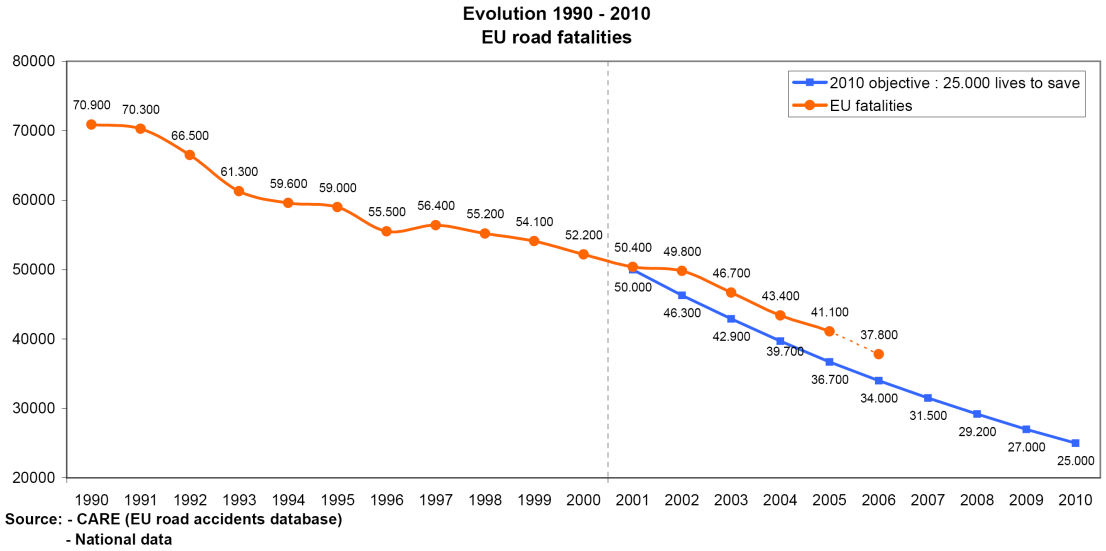

Figure 1.1 Actual evolution and EU objective of road fatalities within the European Union 1990-2010 (European Road Safety Observatory, 2006b).

Vehicle safety can be divided into the two fields active and passive safety. The latter one is the most mature area with the intent to protect the passengers in a vehicle during crash. Passive safety has developed over the last 50 years, whereas during the last decade we have also seen some major advances in the field of active safety, which is aiming at accident avoidance through the use of active systems. Table 1.1 shows when the safety functions common today is activated.

Table 1.1 Active and passive safety functions. (Guillermo & Nilsson, 2006)

<table>
<tr><td colspan="4">Active safety</td><td colspan="3">Passive safety</td></tr>
<tr><td colspan="4">Crash can be avoided</td><td colspan="3" rowspan="4"></td></tr>
<tr><td colspan="3">Driver is in control</td><td>+
Point of no return</td></tr>
<tr><td colspan="2">Driver is fit</td><td>+
Contact</td></tr>
<tr><td>Car is fit</td><td colspan="2"></td></tr>
<tr><td rowspan="2">Seatbelt warning, Navigation, etc</td><td colspan="2">Driver assistance</td><td rowspan="2">Electronic Stability Control, RSC</td><td rowspan="2">Autobrake, Seatbelt pretension</td><td rowspan="2">Energy absorbing structures, Airbags, Whiplash protection</td><td rowspan="2">Event data recorder</td></tr>
<tr><td>Alco-lock, Night vison</td><td>ABS, Traction control, Collision warning</td></tr>
<tr><td>Normal driving</td><td colspan="3">Collision avoidance</td><td>Pre crash</td><td>In crash</td><td>Post crash</td></tr>
</table>

1.1 Passive safety

Passive safety includes technologies that mitigate the damage of a vehicle accident. Typical examples are energy absorbing vehicle structures and passenger restraint systems such as seat belts and airbags. The development and implementation of these systems have been quite successful and for instance in Japan, thanks to passive systems, there has been a decrease in fatalities despite an increase in the number of accidents during the last decade. However, saturation in the effects of passive safety can be seen and therefore a reorientation towards active safety is taking place (Nagai, 2007).

1.2 Active safety

Active safety includes technologies aiming at collision avoidance and improved vehicle handling. This includes functions like Antilock Brake Systems (ABS) and Electronic Stability Control (ESC). More novel active functions used by Volvo Car Corporation (VCC) are Rollover Stability Control (RSC), Driver Alert, and Collision Warning with Brake Support. RSC is an extension to ESC that prevents rollover of vehicles such as the Volvo XC90 and similar SUVs. Driver Alert warns the driver if the driving pattern indicates that the driver is falling asleep. Collision Warning with Brake Support uses radar to determine if there is a risk of impact with a forward vehicle. If such a situation is detected the system warns the driver and pre-charges the brakes. The common factor for these active safety systems is that they focus on helping the driver to keep control of the car in potentially dangerous situations.

1.3 Electronic Stability Control

The most important active safety system is the Electronic Stability Control system. It was introduced to the mass market 1998 and it has shown to reduce the number of crashes since it helps the driver to maintain control of the vehicle during evasive maneuvers. Studies by the American National Highway Traffic Safety Administration (NHTSA) has shown that vehicle crashes are reduced by 35% for passenger cars and 67% for SUVs equipped with an ESC system (Dang, 2004).

Although ESC has had a significant impact on accident statistics, it would not have been possible without earlier implementations of two other technologies developed during the last three decades. The first was the Antilock Brake System (ABS) introduced by Bosch 1978 (Bauer, 1999). The ABS prevents wheel lock and thus preserves the ability to steer the vehicle during full braking (van Zanten, 2002). Although the system is well known and widely spread, studies have not shown that ABS has had a significant effect on accident reduction. Cars equipped with ABS crashes in a different way than cars without the system but the reduction of crashes with injuries is minor. This can be explained by a higher average speed among cars equipped with ABS (Evans, 1998 and Lie, 2005). Traction control systems (TCS) are the second technology. The TCS intervenes by reducing engine torque and by braking when a driven wheel spins due to excessive engine torque. Thus TCS improves the vehicle stability during acceleration, as the ability of a pneumatic tire to transfer lateral force is heavily reduced when spinning.

ESC systems were introduced together with four additional sensors other than those used for ABS and TCS: steering wheel angle, brake pressure, yaw rate and lateral acceleration sensors. Inputs from these sensors are used to compare the vehicle's motion with a reference model, which is used to interpret the driver's intentions. If the vehicle motion deviates from the reference model the ESC intervenes by engine torque reduction and differential wheel braking to introduce a correcting yaw moment (van Zanten, 2002). When doing so, the ESC system utilizes the hardware developed for the ABS and TCS systems.

1.3.1 Over- and understeer interventions

The current Electronic Stability Control systems are designed to make it possible to follow the drivers intended path even though tire forces are saturated due to the limited road adhesion (Wong, 2001). The system is very useful in this situation as the average driver usually does not push the car to its physical limits and the driver is therefore often surprised by the loss of handling performance that can occur during an evasive maneuver or in case of low road-tire friction (van Zanten, 2002).

The ESC helps the driver to keep the intended path by using differential braking of the appropriate wheels. The differential braking results in a stabilizing yaw moment on the vehicle, and the strategy chosen depends on if the vehicle is detected to over- or understeer (Dang 2004). Oversteering means that measured vehicle motion deviates from the driver's intended motion (as interpreted by the reference model) with too much yaw motion. This can be seen in Figure 1.2a below, where the driver intended path is shaded but the actual vehicle cannot manage to follow it as the rear axle has reached its lateral adhesion limit and the vehicle starts to slide sideways. The opposite case is when the vehicle is detected to be understeering, meaning that it is yawing too little and does not manage to keep the driver's intended cornering radius, as seen in Figure 1.2b.

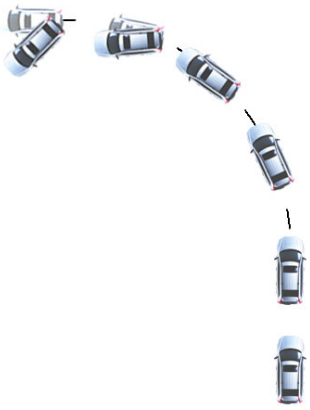

Figure 1.2a Oversteer situation, vehicle yaws too much compared with driver intent.

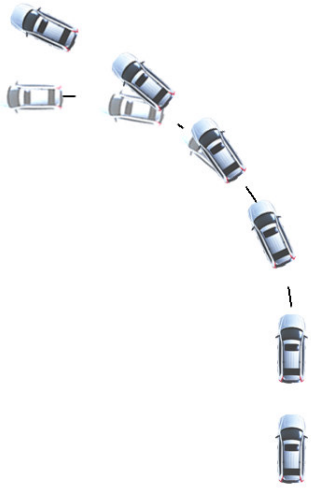

Figure 1.2b Understeer situation, vehicle does not yaw enough compared with driver intent.

In oversteering situations, where the vehicle starts to skid sideways, the front axle has more grip and the greatest yaw rate decreasing response comes from braking the outer front wheel. To further improve the response some ESC systems also use a smaller amount of braking on the outer rear wheel in oversteering situations, see Figure 1.3a. In an understeering situation, where the vehicle is plowing forward in a corner, the rear axle has more grip than the front, and the ESC intervention is therefore actuated using inner rear wheel braking creating additional yaw moment, see Figure 1.3b. Another likely intervention is to limit the engine torque as this can reduce the vehicle speed and help the vehicle through the corner.

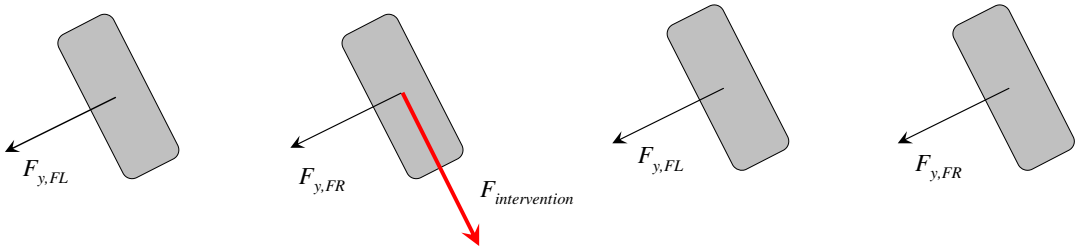

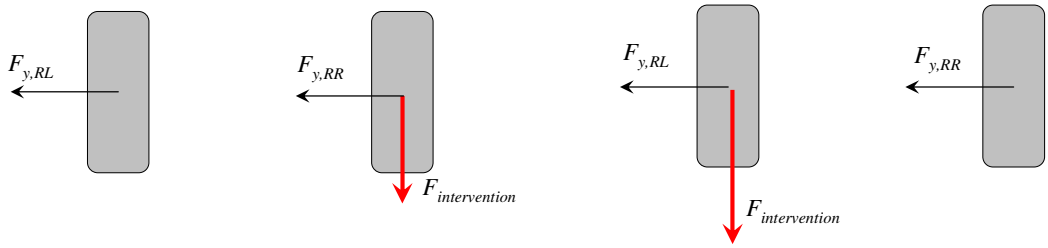

Figure 1.3a Oversteer ESC brake interventions in left turn maneuver.

Figure 1.3b Understeer ESC brake intervention in left turn maneuver.

1.3.2 Alternative approaches

Electronic Stability Control by differential braking is the most frequently used strategy in present systems, but other complementary approaches exist, such as Active Front Steering (AFS) which can correct the vehicle motion by steering the front wheels. AFS is used by for instance BMW and Lexus, and is especially suitable to correct oversteering situations because, as stated in the previous paragraph, the front axle has the most grip and is therefore better suited to generate a correcting torque. Another approach which can be more efficient in understeering situations would be actuation of rear wheel steering, which has been examined by for instance, Håbring (2006).

Other approaches than changing the actuation also exist; Abe et al. (2001) has studied a change in the controlled variable from the vehicle's yaw rate to the side slip angle. The study found it beneficial to control the side slip angle since this parameter better catches the unstable vehicle behavior caused by non-linear tires. As is shown later in this thesis, a vehicle might build up a large side slip angle without an accompanying increase in yaw rate. If so, this may not be detected by the yaw rate based ESC which then does not make any interventions or not enough interventions even though the vehicle is skidding out of control.

Even though it might be beneficial to use side slip angle or rear axle side slip angle as a controlled variable it has not been used in production as it is very difficult to keep track of the vehicle's actual side slip. Two methods to measure or estimate the side slip angle exist, the first method being based on direct integration of the measured lateral acceleration and yaw rate but this method is very sensitive to biased sensors and is likely do diverge as such small measurement errors are integrated (Chumsamutr et al. 2006). The second method is to use an observer, which is a model that from other measured states can give an estimate of the desired variable. Such an approach has been described by for instance Fukada (1999) but both methods are sensitive to disturbances such as road inclination and banking, or in the case of the observer, variations in tire models and surface friction estimations.

1.4 Objective

The objective of this master thesis is to develop a controller that improves existing Electronic Stability Control functions in oversteering situations by adding rear axle side slip control.

- The function should be developed as an addition to existing production like ESC systems. This approach allows us to develop and test rear axle side slip angle control in a short period of time with the possibility to evaluate the developed function in vehicle tests.

- The function should be model based meaning that it is based on a physical data of the controlled vehicle. The intention of this approach is to separate the controller parameters into model parameters which is specific for the current car model and tuning parameters which can be used to adjust the behavior of the function. If the two is separated it will become easier to implement the function in different car models as the model parameters change with the vehicle and only the tuning parameters needs to be tuned. The model based approach should also enable different actuation methods.

- To make the function easily understandable and easy to overview it should be modular and model-based in its structure and implemented in Matlab/Simulink.

1.5 Delimitations

As is described in Section 1.3.2 the estimation of the vehicle side slip or rear axle side slip angle is complicated, but to solve this issue is outside the scope of this Master's Thesis. Therefore, it is assumed that reliable estimates of the side slip and rear axle side slip is available for the developed controller.

Current ESC systems are successful in understeering control, but as stated in the previous Sub-section 1.3.2 it can be insufficient in oversteering situations. It cannot be excluded that added rear axle side slip angle control or combination of a side slip and yaw rate based ESC might be more efficient also in understeering situations. However, this is not treated in this thesis as the major benefit of rear axle side slip control is considered to be in oversteering situations.

The interventions used by the controller are limited to basic oversteering interventions on the outer front wheel. Other more advanced strategies including rear outer wheel braking as depicted in Figure 1.3a or slip control of the braked wheel has not been considered.

Vehicle simulation models might have difficulties to describe the unstable behavior of a vehicle under non-linear slip tire operations, but it is outside the scope of the Master's Thesis to further investigate these issues.

1.6 Procedure

The controller is developed and evaluated using vehicle dynamics simulation software. The software used is called Vedyna and is implemented in a Matlab/Simulink environment. Vedyna uses a complete vehicle model consisting of several different modules for chassis, engine, suspension etc. and can model between 11 and 70 degrees of freedom for the vehicle. In the simulation environment the controller is evaluated using two maneuvers, a so called J-turn maneuver to verify the controllers effect on stability in oversteering situations and a double lane change maneuver to ensure that the vehicle maneuverability is maintained.

As the controller is implemented in Matlab/Simulink it is also possible to use it for rapid prototyping. Using rapid prototyping tools enables us to do vehicle tests to evaluate the developed controller.

2 Vehicle dynamics theory

This chapter contains a brief description of some of the concepts in vehicle dynamics theory for better understanding of active safety functions such as Electronic Stability Control systems.

2.1 Coordinate systems

In the field of vehicle dynamics, notations and coordinate orientations differs somewhat between different authors, but they are mainly based on two conventions; SAE standard SAE J670e (SAE International, 1976) and the international standard ISO 8855 (SIS, 1994). The major difference between the two standards is that the positive z-direction is chosen as upwards from the ground plane in the ISO standard and downwards in the SAE standard, which then gives different directions of the y-axis as the coordinate systems used are right hand oriented. The ISO standard coordinate convention has been chosen as it today is the most common in engineering practice and also used by the simulation tool Vedyna (Tesis Dynaware, 2006b).

The three rotational degrees of freedom for a vehicle is called yaw, pitch and roll. Yaw, ψ, is the angle of rotation around the z-axis which is the result of steering wheel inputs. Pitch, θ, is the angle of rotation around the y-axis, felt particularly when going over a speed bump and finally roll, φ, is the angle of rotation around the x-axis which can be experienced for instance during cornering.

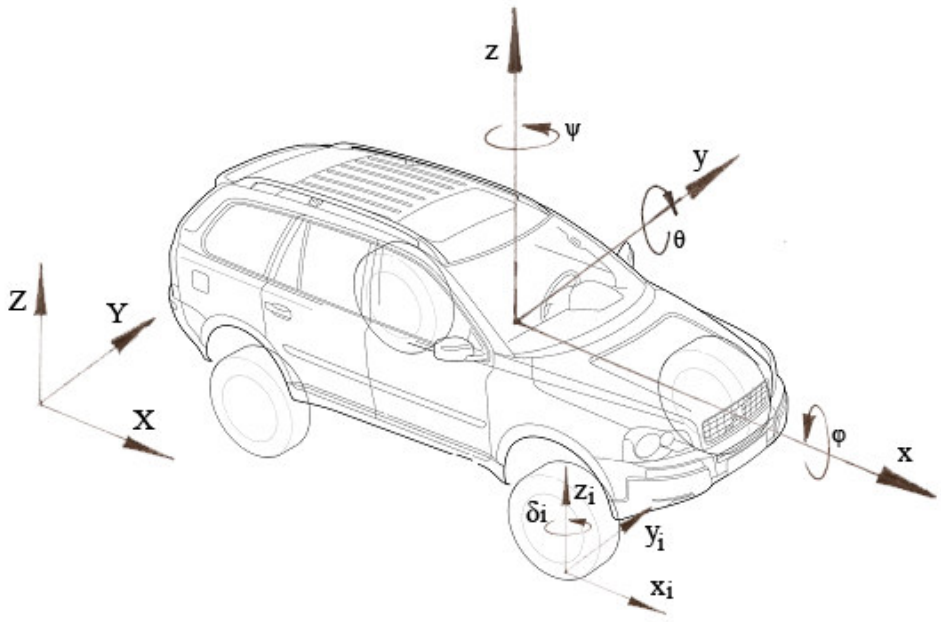

Figure 2.1 Vehicle coordinates in accordance with ISO 8855.

Along with the vehicle centroidal xyz reference frame a global reference frame XYZ is used to describe the vehicle motion with respect to the surrounding environment. For more complex models sometimes wheel fixed coordinate systems are used, with origin in the tire contact patch (Wong, 2001). The degrees of freedom of the tires that might be considered are the rotational speeds ω_i, the vertical displacements z_i and the steer angles δ_i. The subscript *i* is FL, FR, RL, or RR (Front Left – Rear Right) depending on the position of the tire.

2.1.1 Important quantities for vehicle stability control

The most important quantities concerning vehicle stability control are:

-Yaw rate, $\dot{\psi}$

The yaw rate is the time derivative of the yaw angle. This quantity is possible and inexpensive to measure and is therefore frequently used in modern cars to activate the electronic stability control function (Piyabongkarn et al. 2006). The drawback of only using this quantity is the lack of possibility to detect side slip angles building up at a slow rate.

-Vehicle side slip angle, β

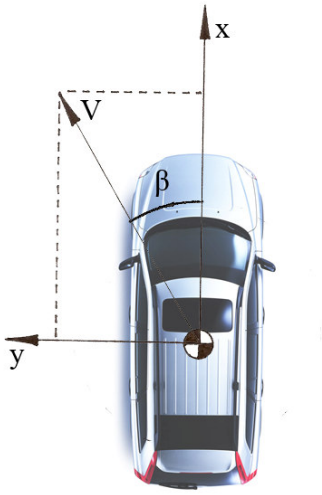

Figure 2.2 Vehicle side slip angle.

The vehicle side slip angle (SSA) is defined as the angle between the vehicles fixed x-axle and the vehicle velocity at center of gravity

$$\beta = \arctan\left(\frac{V_y}{V_x}\right). \tag{2.1}$$

The side slip angle exists due to the fact that the vehicle's resulting velocity vector is not always in the heading direction of the vehicle. The vehicle side slip angle can also be measured for instance at the rear axle and would then include a term depending on the yaw rate as the vehicle body is also rotating. The vehicle side slip angle at the rear axle (SSRA) is then equal to the tire slip angle of the rear wheels which will be discussed in the next chapter.

2.2 Tires

When considering vehicle handling and performance, the tires are the most important component of the vehicle as only the tires are in contact with the road and can transfer force between the road and the vehicle.

2.2.1 Longitudinal tire forces

For longitudinal tire forces, consider that a driving torque is applied to the wheel. As the rubber tire is non rigid, the vertical force (i.e. the weight of the vehicle) forces the tire to be in contact with the ground over an area. The driving torque then causes the tire to deform and it partially starts to slip in the contact patch (Wong, 2001). This means that the tire longitudinal force is transferred both through adhesion and slipping of the contact patch, and the force transferred is proportional to the amount of slip taking place, and typically the longitudinal tire force is presented as a function of tire slip and normal load on the tire.

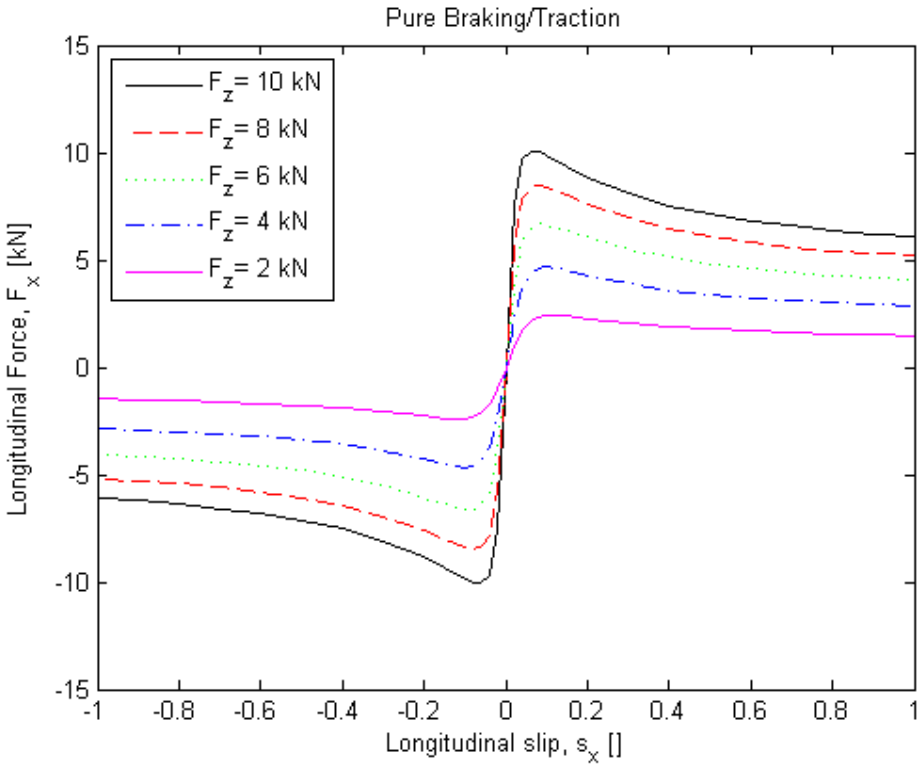

Figure 2.3 Longitudinal tire force for a given slip and normal load F_z.

To be able to match the curves in Figure 2.3 the definition of slip needs to be different depending on if the tire is braking or accelerating. The following definition are used to compute the slip of a tire

$$s_{xi} = \begin{cases} \dfrac{R\varpi_i - V_{xi}}{|R\varpi_i|} & acceleration, \\ \dfrac{R\varpi_i - V_{xi}}{|V_{xi}|} & braking. \end{cases} \tag{2.2}$$

The reason for using different ways to compute the slip for a braking or accelerating wheel is to avoid numerical problems (division by zero) as a free spinning tire during acceleration can have zero longitudinal speed and a locked tire during braking can have zero rotational speed. The longitudinal tire slip – force curve in Figure 2.3 also shows one of the purposes of TCS systems which try to limit the slip to keep the tire working at absolute values below the peak where $s_x \approx 0.07$ where the most traction force can be transferred for this tire.

2.2.2 Lateral tire forces

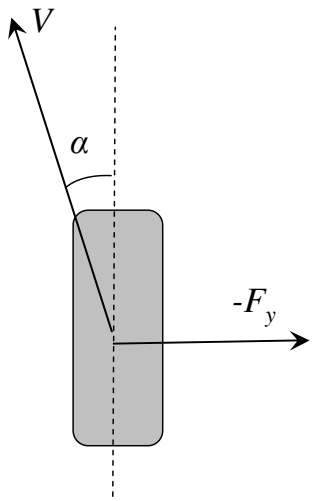

Figure 2.4 Positive tire slip angle α and accompanying negative lateral force F_y.

A similar approach as for the longitudinal tire force is used to determine the lateral force generated by a tire. If the heading direction of the tire differs from its travel direction, the angle in between is called the tire slip angle and a lateral force proportional to the slip angle of the tire tries to align it in the travel direction. The dependency of the lateral force on the slip angle and normal load on the tire can be seen in Figure 2.5.

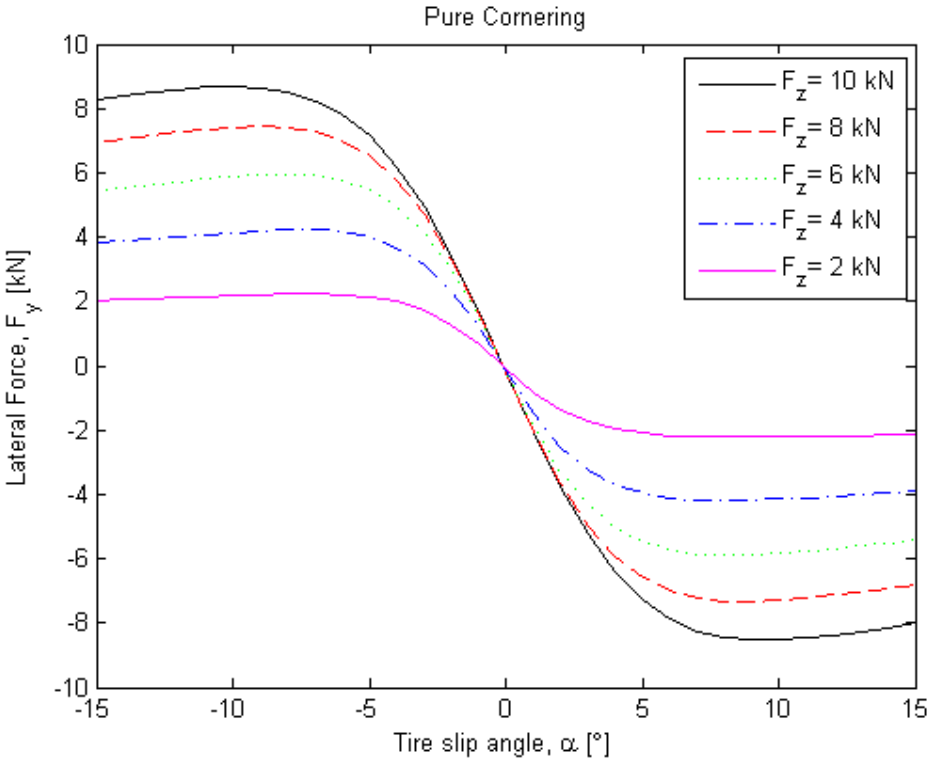

Figure 2.5 Lateral force as function tire slip angle and normal load F_z.

If the lateral force is considered as a frictional force which counteracts the sliding movement in the tire contact patch we get the relation seen in Figure 2.5 above, where negative slip angles give a positive lateral force in accordance with ISO 8855. The definitions of the slip angles are then, if we make the appropriate small angle approximations and only consider the average for the front and rear axle

$$\alpha_f = \frac{V_y + l_1\dot{\psi}}{V_x} - \delta_f \,, \tag{2.3}$$

$$\alpha_r = \frac{V_y - l_2\dot{\psi}}{V_x} \quad . \tag{2.4}$$

In the equations above l_1 represents the distance between the front axle and the vehicle CoG, analogously l_2 the distance to the rear axle, and finally δ_f is the average steering angle of the front wheels.

2.2.3 Combined lateral and longitudinal tire forces

The figures of lateral and longitudinal forces above only show the relation to pure lateral slip angle and longitudinal slip, but as a tire is subject to a combination of lateral and longitudinal slip the maximum force in each direction decrease as the amount of available friction is limited. This is sometimes referred to as the friction circle, or friction ellipse, which gives a relationship between the maximum F_x and F_y (Pacejka, 2002). Figure 2.6 below shows how the maximum lateral force is decreased for increasing longitudinal slip. This relation between the maximum lateral force that can be generated and the longitudinal slip is the reason to why ABS and TCS are used. The ABS limits the longitudinal wheel slip during braking, enabling the tire to also develop lateral forces which then allows for the driver to steer the vehicle during maximum braking, and TCS allows for the driver to steer when accelerating.

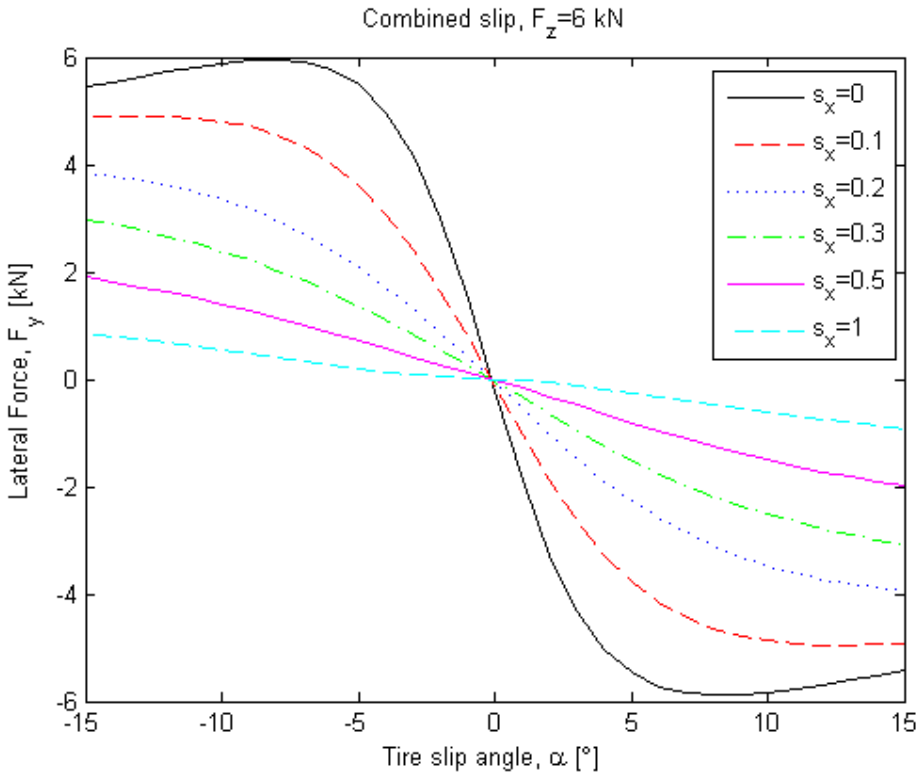

Figure 2.6 Combined slip influence on lateral force.

2.2.4 Tire modeling

The force transfer between tire and road described in the previous paragraphs is complex and no complete theoretical model exist. Instead tire test data is used to produce curve fits in empirical models, and one of these is the Magic Formula (Pacejka, 2002) which in its general form read

$$Y(x) = D\sin\left[C\arctan\left\{Bx - E\left(Bx - \arctan(Bx)\right)\right\}\right]. \tag{2.5}$$

In Equation 2.5 $Y(x)$ is either $F_x(s)$ or $F_y(\alpha)$. The coefficients B (Stiffness factor), C (Shape factor), D (Peak value) and E (Curvature factor) are determined through tire testing which can be quite expensive, why tire data is not commonly made available for public use. Some of these parameters impact on the tire model can be seen in Figure 2.7.

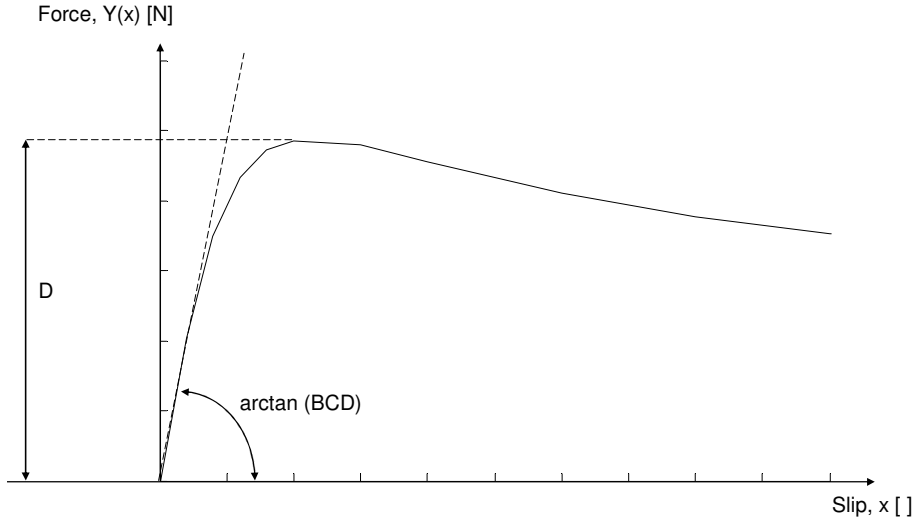

Figure 2.7 D=Peak value. BCD= Cornering stiffness when $Y=F_y$.

The Magic Formula version called Delft-Tyre 1996 is implemented in the Vedyna vehicle model used in this thesis. The tire data are collected from Michelin Diamaris 235/60 R18 tires. Figures 2.3 and 2.5-2.6 display some of the characteristics of the used tires.

In more basic models, such as the 3-DOF Bicycle model described below, a simplified approach is sometimes used, namely a linear tire model where the longitudinal and lateral force is directly proportional to the slip and slip angles so that:

$$F_y = -C_\alpha \alpha, \tag{2.6}$$

$$F_x = C_s s_x. \tag{2.7}$$

This assumption is valid for small slip values and angles, as the longitudinal tire stiffness (C_s) and the cornering stiffness (C_α) corresponds to the slopes around the origin in Figures 2.3, Figure 2.5 and the dashed line with slope arctan(BCD) in Figure 2.7.

2.3 The Bicycle model

A simple and frequently used vehicle dynamics model is the three degrees of freedom (3-DOF) vehicle model commonly called the Bicycle model. The model's name comes from the assumption that the track width of the vehicle can be neglected with respect to the cornering radius, making it possible to model the vehicle with only one front and one rear tire with the combined lateral stiffness of both tires on the respective axle. The model also neglects the roll and pitch rotations as well as the vertical translation degree of freedom. Furthermore, the tire slip angles are assumed to be small so that cos α = 1 and sin α = α.

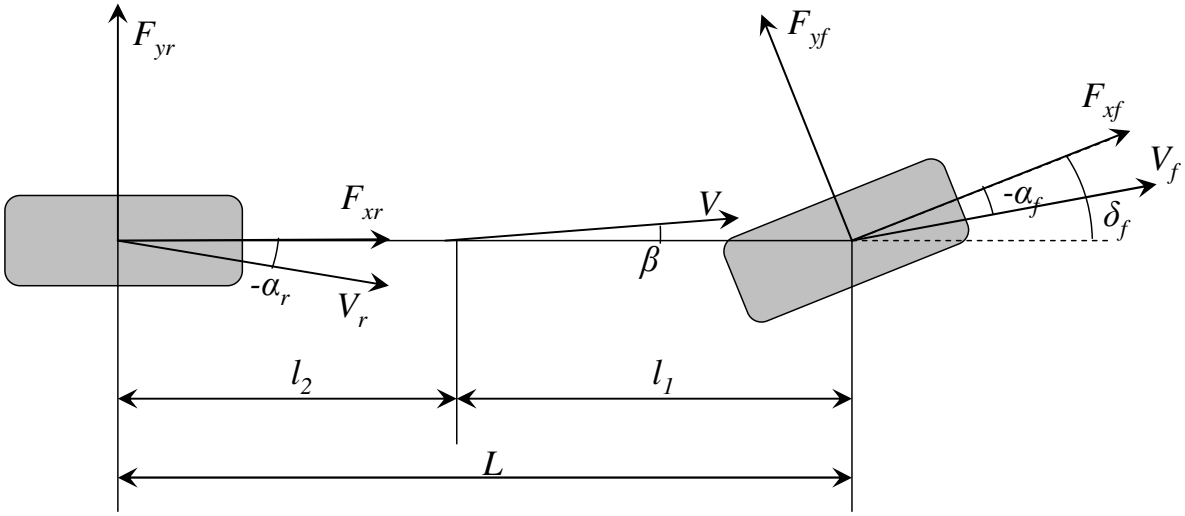

Figure 2.8 The Bicycle model. Positive lateral forces for negative slip angles in accordance with Equation 2.6.

Based on the assumptions above the equations of motion for the Bicycle vehicle model is (Wong, 2001)

$$m \cdot \left(\dot{V}_x - \dot{\psi} \cdot V_y\right) = F_{xf} + F_{xr} - F_{yf} \cdot \delta_f \,, \tag{2.8}$$

$$m \cdot \left(\dot{V}_y + \dot{\psi} \cdot V_x\right) = F_{yr} + F_{yf} + F_{xf} \cdot \delta_f \,, \tag{2.9}$$

$$I_z \ddot{\psi} = l_1 \cdot F_{yf} - l_2 \cdot F_{yr} + l_1 \cdot F_{xf} \cdot \delta_f \,. \tag{2.10}$$

If the lateral and longitudinal forces are given by Equations 2.3-2.4, and 2.6-2.7 the model can be referred to as being linear because of the force-slip relation assumption in Equations 2.6 and 2.7. This assumption is made for the reference model used in the controller described in Chapter 3.

2.4 Vehicle stability

In control theory many definitions of stability exists, but in case of non-linear systems such as a vehicle with non-linear tires it is not possible to analytically analyze the stability (Kiencke & Nielsen, 2000). To solve this issue, in this thesis a vehicle is considered as stable if the driver is still able to control the vehicle. In the terms of side slip angle, driver loss of control occurs when the tire lateral force has passed its peak, which would be at approximately 15° on high friction surfaces and decreasing down to 4° on low friction surfaces such as packed snow (van Zanten, 2002).

One of the central concepts for electronic stability control is that of over- and understeering as it describes how the vehicle deviates from the driver's intended yaw rate. Over- and understeering is also in another context concerning more traditional vehicle dynamics. The basic handling properties of a vehicle without active systems can be described in the terms of over- or understeer and one then refers to the steady state cornering properties of the vehicle.

An oversteer vehicle has a larger slip angle on the rear axle ($|\alpha_r| > |\alpha_f|$) and an understeer vehicle has a larger slip angle on the front axle ($|\alpha_f| > |\alpha_r|$). It can be shown that the steer angle required during a given steady state cornering can be written as (Wong, 2001)

$$\delta_f = \frac{L}{R} + \alpha_f - \alpha_r = \frac{L}{R} + \frac{F_{yf}}{C_{\alpha f}} - \frac{F_{yr}}{C_{\alpha r}}. \tag{2.11}$$

where Equation 2.6 is used for the relation between slip angle and lateral force. The lateral acceleration is given by the sum of the lateral forces in accordance with Newton's second law and the utilized friction can be written as the ratio between the lateral acceleration (a_y) and the normal acceleration (g)

$$F_{yi} = W_i \mu = W_i \frac{a_y}{g} = W_i \frac{V^2}{gR}. \tag{2.12}$$

Inserted in Equation 2.11 this gives

$$\delta_f = \frac{L}{R} + \frac{W_f}{C_{\alpha f}} \frac{V^2}{gR} - \frac{W_r}{C_{\alpha r}} \frac{V^2}{gR}, \tag{2.13}$$

where the understeer coefficient is defined as

$$K_{us} = \frac{W_f}{C_{\alpha f}} - \frac{W_r}{C_{\alpha r}}, \tag{2.14}$$

and this gives

$$\delta_f = \frac{L}{R} + K_{us} \frac{V^2}{gR}. \tag{2.15}$$

In the equations above δ_f represents the steering angle of the front axle, L is the vehicle wheel base, R the cornering radius, and V the longitudinal speed of the vehicle. W_f and W_r is the static vehicle weight on the front and rear axle, respectively.

For a constant steer angle δ_f; a vehicle that has an understeer coefficient K_{us} equal to zero, will continue on the same turning radius even if the longitudinal speed is increased. If K_{us} is smaller than zero the vehicle is said to be oversteered and this will cause the vehicle to get a smaller turning radius as speed is increased with the same steering angle. If K_{us} is larger than zero the vehicle will increase its turning radius and is therefore said to be understeered.

As vehicles that are oversteered experiences directional instabilities at certain velocities most production cars are designed to be understeered (Wong, 2001). However, the suspension design of a vehicle might be such that for certain conditions, such as high lateral accelerations, the understeer characteristics of the vehicle might increase or decrease. A typical property that will affect the understeer is the roll stiffness distribution between front and rear axle. It is common to have a higher roll-stiffness in the front than in the rear, which causes the relative load transfer from inner to outer tire to be larger in the front. A more evenly spread weight distribution on an axle gives a higher effective lateral axle stiffness because of the tire characteristics, and the effective lateral axle stiffness then decreases more in the front than in the rear, making the vehicle more understeered in the case of high lateral accelerations (Jacobson).

An action that can cause the vehicle to be more oversteered instead is if a load transfer occurs from the rear to the front, for example as the result of driver braking or accelerator pedal release. The change in normal load affects the cornering stiffness, as can be seen in Figure 2.5, and the distribution of the lateral force might become such that the vehicle oversteers into the curve, building up a large rear axle side slip angle (Andreasson, 2007).

2.4.1 Phase portraits for stability analysis

If a vehicle is doing a turn in which the longitudinal speed and steering wheel angle is constant, it will after some time reach a steady state condition where the yaw rate and lateral velocity is constant. The state that the vehicle approaches is depending on the properties of the tires and the suspension mounted on the car, or in the case of the Bicycle model, the lateral stiffness distribution between the front and rear axle. A way to visualize the steady state point is to use a phase portrait plot of the two states against each other. Figure 2.9 below shows the response of the Vedyna simulation model for a steering wheel angle step of 40 ° at a constant longitudinal speed of 150 km/h.

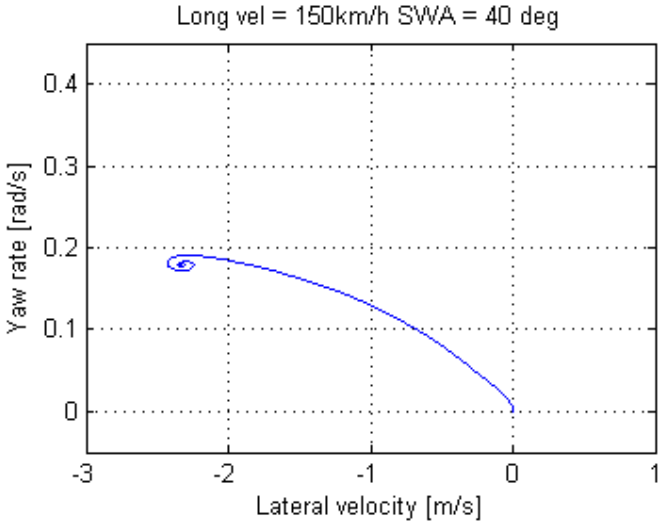

Figure 2.9 Yaw rate and lateral velocity for a vehicle entering a steady state cornering at 150 km/h with a 40° SWA ramp.

If the vehicle is disturbed from its steady state either by outside influence or driver actions such as an accelerator pedal release, it will follow a trajectory in the phase plane depending on the current distribution of the lateral forces. If the disturbance is minor the vehicle will soon regain its normal lateral force distribution and return to a steady state. However, if the disturbance is large enough the vehicle might not be able to return to a stable state and therefore the driver might loose control of the vehicle. This can for instance be seen in Figure 2.10 where an accelerator pedal release leads to loss of vehicle control and a very large lateral velocity, which is equivalent to a large side slip angle. To prevent situations like this is the principal purpose of ESC systems, which does interventions based on the vehicle's yaw rate deviation from a reference value. In Figure 2.10 an intervention by the ESC would try to limit the yaw rate seen on the y-axis to keep it below a certain threshold level.

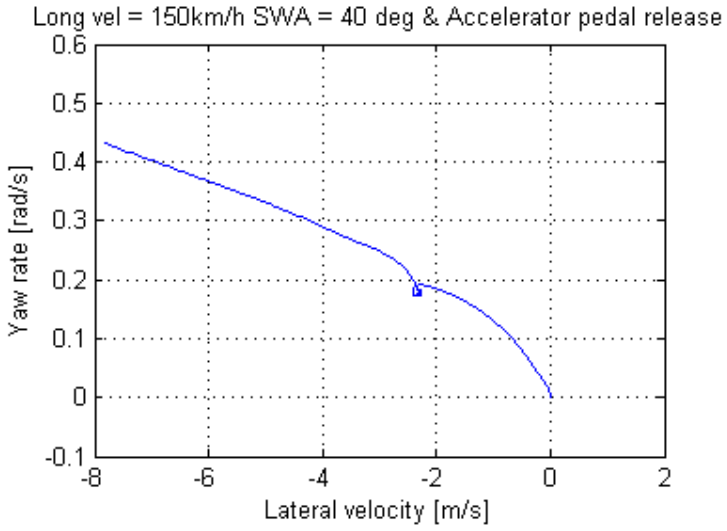

Figure 2.10 Accelerator pedal release in the steady state cornering seen in Figure 2.9.

Figure 2.9 and 2.10 show the trajectory of the vehicle states for the more advanced Vedyna simulation model, but to visualize the effects of a load transfer like that of the previously described accelerator pedal release, the simpler Bicycle model is useful. If the first equation of the Bicycle model is neglected by assuming that the driving force needed to maintain constant longitudinal speed is small enough to not affect the lateral force generation, the coupled Equations 2.9 and 2.10 can be numerically solved the for different initial conditions $\dot{\psi}_0$ and V_{y_0}. The trajectories of the numerical solutions to the equations then show how the vehicle would respond if subject to an external disturbance.

The yaw rate and the lateral velocity is related to the slip angles through the Equations 2.3 and 2.4, and as the longitudinal speed and steering angle is held constant in the phase portrait the front and rear axle slip angles make up a new set of coordinate axes in the phase plane given by

$$\frac{V_y - l_2\dot{\psi}}{V_x} = \alpha_r = 0 \Leftrightarrow \dot{\psi} = \frac{V_y}{l_2} \tag{2.16}$$

and

$$\frac{V_y + l_1\dot{\psi}}{V_x} - \delta_f = \alpha_f = 0 \Leftrightarrow \dot{\psi} = \frac{\delta_f V_x - V_y}{l_1}. \tag{2.17}$$

The trajectories that the Bicycle model with pure understeer axle characteristics would follow if disturbed from its steady state is shown in Figure 2.11. The gradient markers show the direction along the trajectories in which the vehicle would be moving. The rotated coordinate axes represent the given states current slip angles in accordance to Equations 2.16 and 2.17 above.

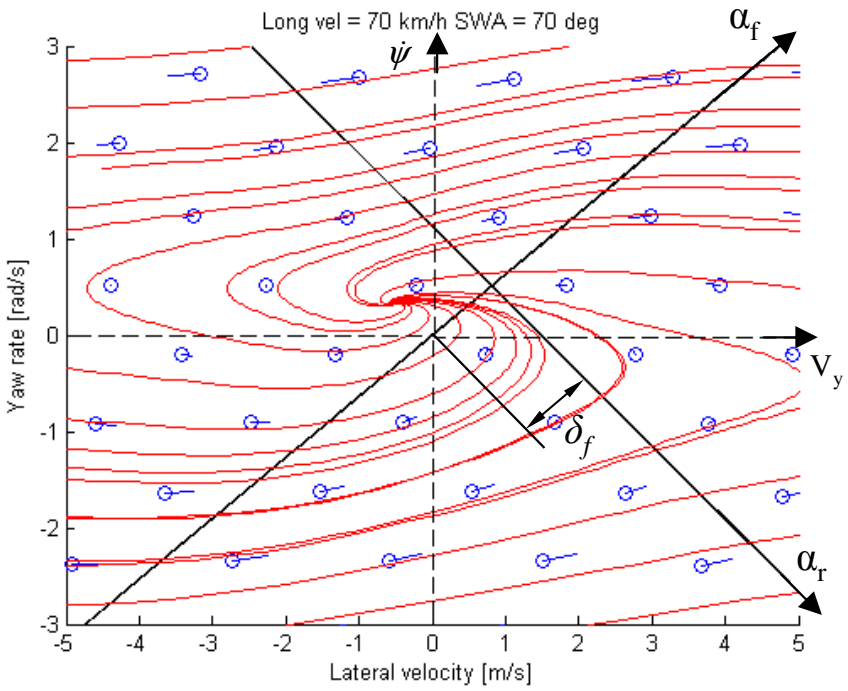

Figure 2.11 Phase portrait for understeered vehicle (K_{us} >0). Gradient markers show the travel direction along the trajectories. Rotated coordinate axes represent front and rear slip angles, with α_f displaced from the origin because of the steering angle δ_f.

2.4.2 Load transfer effect in the phase portrait

As can be seen in Figure 2.11, the vehicle will return to the steady state point along the trajectories in the figure after a disturbance to another state, and this behavior is typical for the stability of the understeered vehicle. However, in our case we don't have an external disturbance in the form of an impulse force or moment, but instead the cornering properties of the vehicle is changed why it is of interest to study how such change in cornering stiffness distribution and understeer coefficient affects the vehicle's phase portrait.

The load transfer from rear to front axle changes the distribution of the cornering stiffness, which momentarily can make the vehicle oversteer. The resulting phase portrait for such conditions can be seen in Figure 2.12 below where the cornering stiffness distribution of the vehicle has been changed so that $K_{us}<0$.

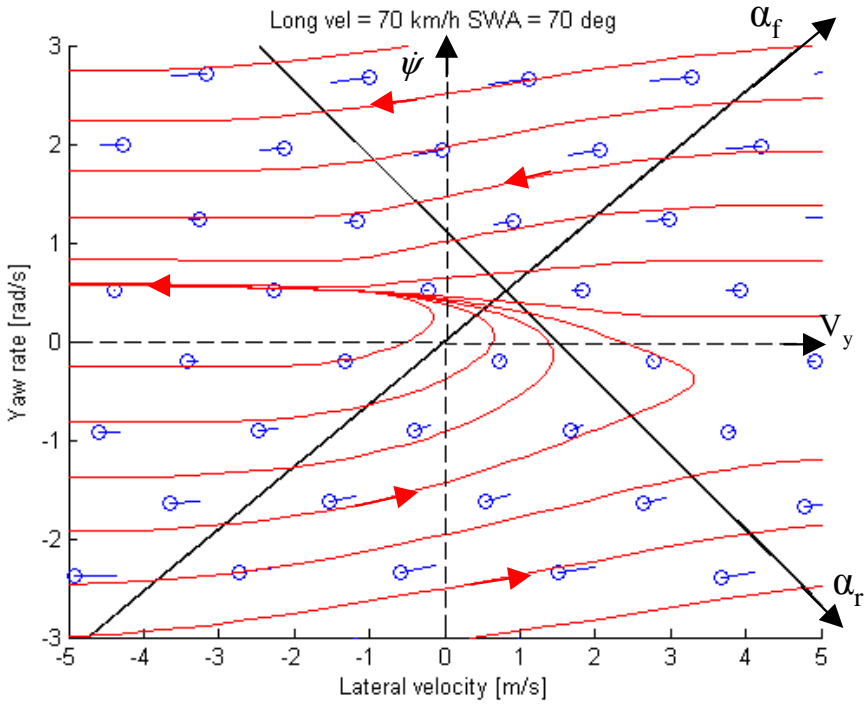

Figure 2.12 Phase portrait for vehicle with load transfer toward front axle so that $K_{us}<0$.

As can be seen in Figure 2.12 the vehicle no longer has a steady state point under the current conditions and will follow a trajectory which leads to a large increase in lateral velocity. This increase in lateral velocity means that the side slip angle is growing, which is likely to become a problem for the driver. The conventional ESC can handle this if there is also an increase in the yaw rate, but adding side slip control can make it possible to do earlier interventions and handle the cases where there is no significant increase in yaw rate. It should be noted that Figure 2.12 is an exaggeration of the possible vehicle behavior, and that the trajectories assumes that the longitudinal speed is constant, which would not be the case if the vehicle starts sliding sideways. However, it clearly shows the tendency of how the vehicle responds to the load transfer and that the increase in yaw rate is minor even though the side slip is growing.

2.4.3 Electronic Stability Control yaw rate thresholds

If we use the phase portraits to study ESC interventions we can see that the upper left area in Figure 2.13 below corresponds to oversteering interventions as the yaw rate is too high compared with a reference state that would be adjacent to the point where the trajectories coincide. The lower left area would correspond to understeering interventions and the corridor in between the two areas is where the vehicle might be wandering off without the yaw rate based ESC making interventions or too small interventions as the yaw rate error is small. The size of the corridor, or the dead band, is part of the tuning of the controller. If it is too small ESC would be doing too frequent interventions which would cause excessive wear to the actuators (the brakes) and also impair the experienced drivability of the vehicle. The opposite would of course not be accepted either as the ESC would be unable to aid the driver when needed.

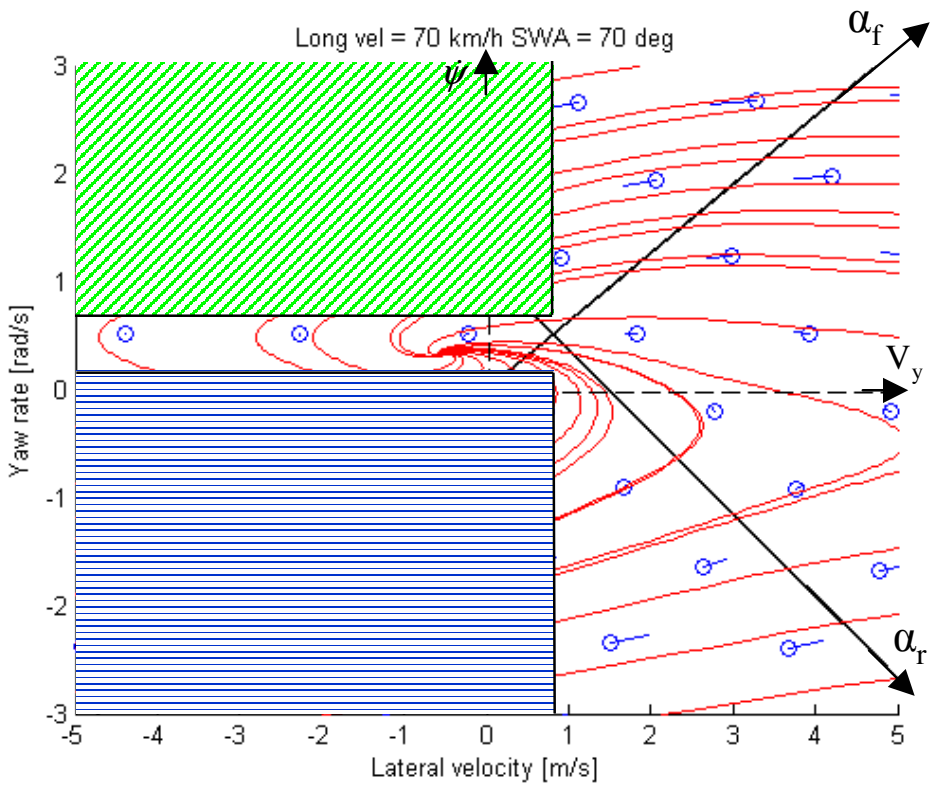

Figure 2.13 ESC interventions in the phase-plane. In the upper left area the vehicle is considered to oversteer and in the lower left to understeer.

2.4.4 Rear axle side slip control threshold

As is described in chapter 1.3.1 the ESC intervenes in oversteering situations where the vehicle is detected to have a too high yaw rate by braking the outer wheels. The change in the vehicle behavior to become less understeered because of a load transfer from the rear to the front axle is also an oversteer situation, and as seen in the previous figures it can be undetected or underestimated by the ESC as the yaw rate increase is not large enough. Adding rear axle side slip control would introduce a new control threshold in the phase-plane, which would have a border parallel to the α_f axis as indicated in Figure 2.14. As too large rear axle slip angles is equal to oversteering situations, the interventions should be limited to front outer wheel braking and the control area would stop where the ESC indicates understeering.

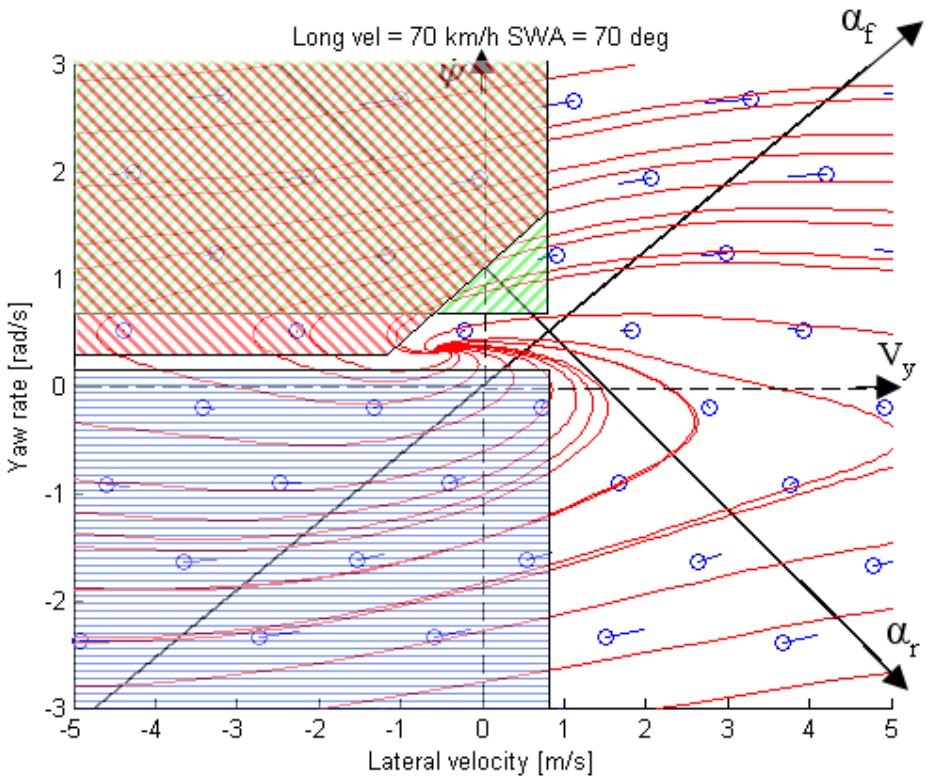

Figure 2.14 Added SSRA control threshold in the phase portrait.

2.4.5 Oversteering interventions shown in the phase portrait

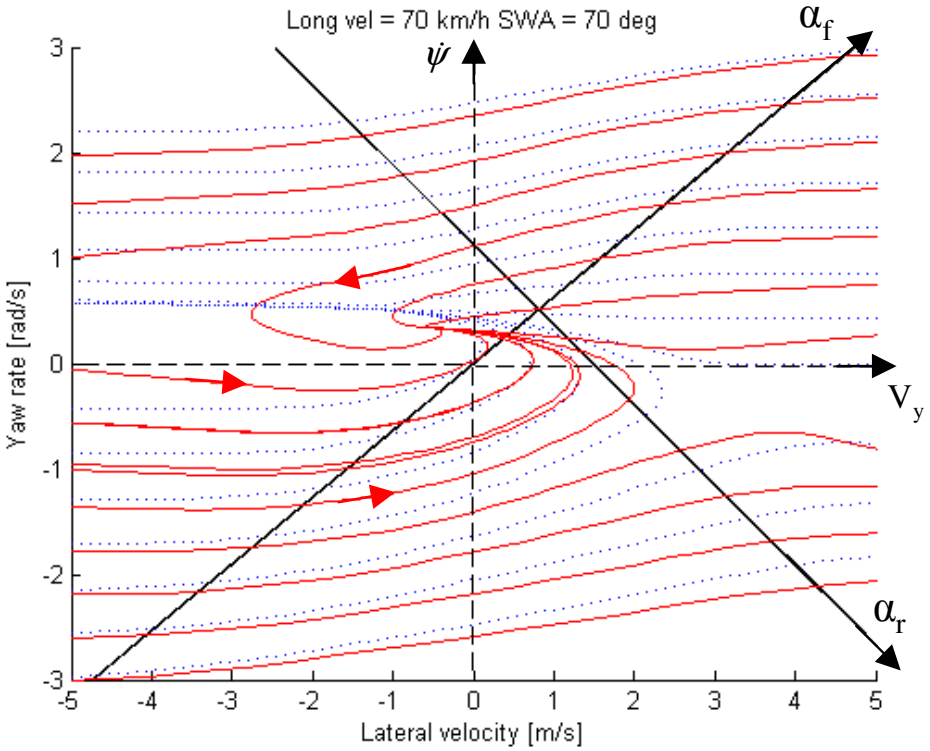

Figure 2.15 Trajectories in the phase-plane during the influence of oversteering interventions.

Figure 2.15 reconnects to Figure 2.12 as the trajectories of the oversteered vehicle can be seen as the dashed lines. The solid lines in the figure represent the development of the vehicle states under the influence of an extra correcting yaw moment due to a brake intervention on the outer front wheel. As can be seen in the figure the vehicle regains its normal stable behavior and returns to a steady state point along the solid trajectories. How steep the curves back to the steady state point are depends on the size of the brake intervention.

The discussion above would explain how a situation where a too large lateral velocity (side slip angle) can be solved by making an intervention in a direction orthogonal to the actual control variable (the brake force is in the longitudinal direction compared with the lateral velocity that is represented by the side slip angle). As the outer tire is braking and a correcting yaw moment is generated, the side slip angle decreases and the vehicle states will then follow a trajectory in phase plane back to a new steady state.

3 Controller design

As is stated in Section 1.3.1 the average driver does not usually use the vehicle outside the linear range of operation and might be surprised of the non-linear vehicle behavior described in Section 2.4. As the driver might not be able to handle the vehicle in such a situation it can be said that the stability of the vehicle is lost even though it is equipped with a yaw rate based ESC system. It is therefore the objective of the side slip at the rear axle (SSRA) controller to ensure that the rear axle side slip is limited so that the vehicle's linear behavior, which can be considered stable for the driver, is maintained. The controller should be implemented in such a way that the model parameters that change with the current vehicle model is separated from tuning parameters which is used to adjust the controller behavior.

3.1 The reference model

The basis for the rear axle side slip controller is a reference model to which the vehicle's actual or estimated side slip at the rear axle is compared. The reference model gives an upper limit of what rear axle side slip angle that can be allowed in different driving situations, and as the vehicle behavior should be predictable for the driver the linearized Bicycle model described in Section 2.3 is suitable as a reference model.

The Bicycle model is also commonly used as a reference model for yaw rate based ESC functions, but then with certain delimitations, such as limiting of the maximum target yaw rate based on an estimation of the available friction (van Zanten, 2000). A major difference between the SSRA controller and the regular ESC is that the SSRA controller is designed to only act when oversteering is detected whereas the ESC acts in both understeering and oversteering situations. This influences the objective of the reference model in such a way that the target value in the SSRA controller case is used only as an upper limit which the SSRA may not exceed. This approach makes it possible to tune the reference model so that it allows more or less rear axle side slip, adding a tuning parameter to the reference model for the cornering stiffness values $C_{\alpha f}$ and $C_{\alpha r}$. The rest of the parameters for the reference model are model parameters such as vehicle mass m, yaw moment of inertia I_z, and axle distances l_1 and l_2.

The reference model is only used to study the vehicle's lateral behavior why it is possible to use the actual vehicle longitudinal velocity as input and neglect Equation 2.8. For yaw rate control Equation 2.10 is the most interesting one, but as we are interested in the rear axle side slip angle the lateral velocity Equation 2.9 is also significant. As the equations are coupled both needs to be solved to generate the allowed SSRA upper limit, which is calculated from the reference model's yaw rate and lateral velocity in Equation 2.4. As the wheels on the rear axle cannot be steered the side slip angle on this axle is equivalent to the tire slip angle calculated in Equation 2.4.

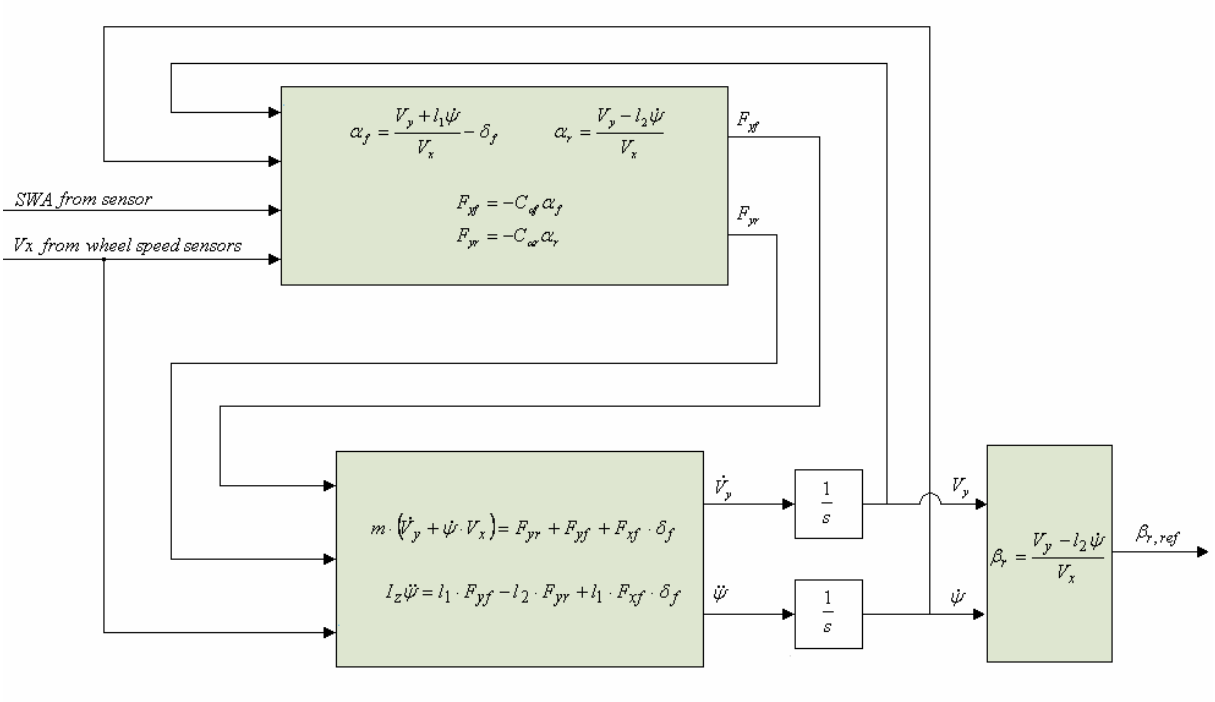

Figure 3.1 Reference model. The reference rear axle side slip angle is calculated through Equation 2.4 with the yaw rate and lateral velocity from the reference model.

Figure 3.1 shows how the reference model takes in sensor signals of the steering wheel angle and the longitudinal vehicle speed to solve Equation 2.9 and 2.10. The reference model states given by these solutions follow the actual vehicle behavior well if the front and rear axle characteristics resemble that of the real vehicle and as long as the maneuver is such that the tires stay at small slip values, where their characteristics is almost linear. This can be seen in Figure 3.2 where the vehicle side slip and rear axle side slip is plotted together with the more complex Vedyna vehicle model.

3.2 Reference model tuning

As the reference model uses a linear tire model, the tire forces will always increase with increasing slip angles and thus making the reference model more stable than a real vehicle. However, this is a desired effect, as the normal driver usually does not drive outside the linear limit of the vehicle's handling range (van Zanten, 2000). The parameters used for the reference model are quite easy to derive as they mostly consist of vehicle data such as vehicle mass and inertia. The cornering stiffness values on the other hand is more difficult as the influence of the suspension geometry change the effective axle characteristics depending on lateral acceleration etc. As the cornering stiffness values are constant for the Bicycle model we need to find a compromise that gives a desired reference value under varying conditions.

If the cornering stiffness in the Bicycle model is tuned so that the vehicle is neutral steered, larger rear axle side slip values are allowed in a double lane change (DLC) maneuver. This solves a problem that can be experienced if not enough rear axle side slip is allowed by the controller, making the SSRA controlled vehicle heavily understeer. However, it is also problematic to use the neutral steer cornering stiffness data for the reference model as it has to be valid over a large range of velocities, and for increasing velocities the reference and the actual vehicle diverge more and more as the understeered real vehicle gets a larger turning radius for a given steering wheel angle when the longitudinal velocity increases.

As can be seen in Figure 3.2, if one considers the rear axle side slip β_r, which is equivalent to the tire slip angle α_r for the 3-DOF Bicycle model, the reference model follows the real vehicle better in the double lane change as well as in the J-turn maneuver than if the side slip angle is considered. It is also a more suitable as a control variable as it directly relates to the oversteering problem that we are trying to solve, as we want to prevent large side slip angles by avoiding sliding of the rear axle. The rear axle side slip is also more directly connected to the yaw rate which we can affect through Equation 2.4 by braking the front tires. Therefore, it is better to use the side slip angle at the rear axle as the control variable than the side slip angle.

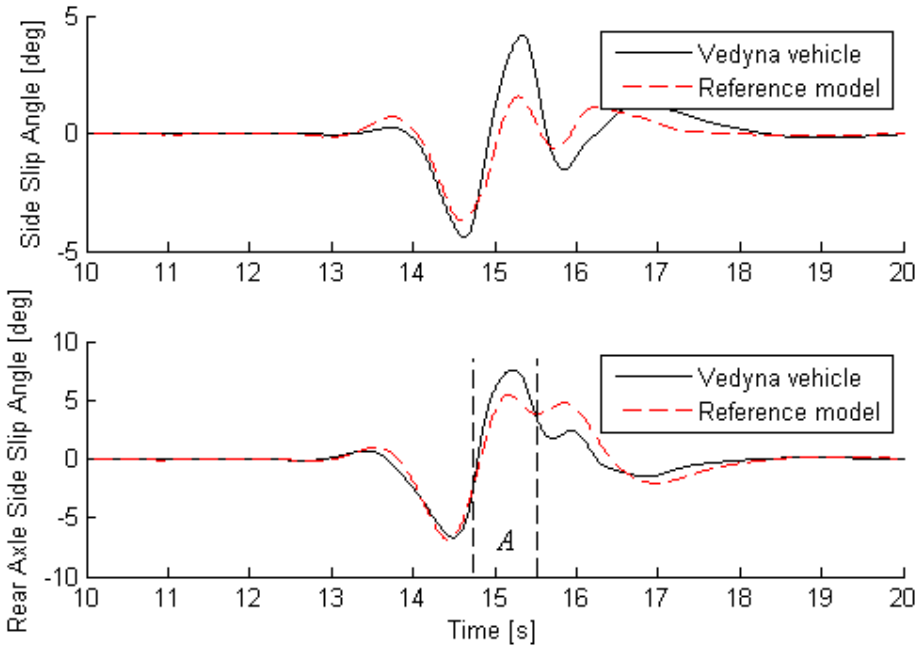

Figure 3.2 Reference model and Vedyna vehicle model in a successful double lane change at 63 km/h with ESC active. Section A shows where the SSRA controller would intervene because of the excessive rear axle side slip.

If we want to tune our model to be more forgiving and allow more rear axle side slip in the DLC maneuver, the simplest way is to adjust the distribution of the cornering stiffness from rear to front, making the model less understeer which is desirable to prevent the vehicle from plowing through a double lane change maneuver. However, this tuning cannot be pushed to far as it desensitizes the controller in the J-turn maneuver as it then allows more side slip before intervention. In conclusion, the reference model should be tuned so that it is a little bit less understeered than the controlled vehicle to allow normal operation without interventions and correct interventions in dangerous situations. As seen in Figure 3.2 interventions will only occur in a short period of time around 15s (*A*) if only excessive side slip at the rear axle is studied.

3.3 Controller model

The developed SSRA controller is a proportional controller that is implemented in Matlab/Simulink and the Simulink model can be seen in Appendix A, Figure A1. The controllers structure is determined by the data flow in Simulink but can also be explained by the following logic description.

The input to the controller is the reference value generated by the Bicycle model, $\beta_{r,ref}$, and the measured or estimated rear axle side slip angle, β_r. The two are compared and the error e between them is calculated

$$e = \beta_r - \beta_{r,ref} \cdot \tag{3.1}$$

The controller should only intervene in oversteering situations where actual rear axle side slip is larger than that of the reference model. This is ensured by comparing the sign of the error with the sign of the rear axle side slip. If the two have the same sign, the actual SSRA is larger than that of the reference model and a yaw moment request $T_{z,req}$ proportional to a controller gain K_p is calculated

$$T_{z,req} = \begin{cases} K_p \cdot e & sign(\beta_r) = sign(e), \\ 0 & sign(\beta_r) \neq sign(e). \end{cases} \tag{3.2}$$

The controller gain K_p is the most important tuning parameter of the controller and has the unit Nm/rad. The yaw moment request is actuated by the outer front brake, why it is necessary to translate the yaw moment request to an appropriate brake pressure request

$$P_{req} = G \cdot T_{z,req}, \tag{3.3}$$

where

$$G = \frac{R_{wheel}}{R_{disc} A_{pad} \mu_{disc} w}. \tag{3.4}$$

Here the constant G transforms the yaw moment request to a brake pressure by scaling with the model parameters for the current vehicle's properties. The model parameters in Equation 3.4 above is the front wheel radius R_{wheel}, the effective brake disc radius R_{disc}, the brake pad area A_{pad}, the friction coefficient between brake disc and pads μ_{disc}, and finally the track width w of the vehicle.

The brake pressure should be applied on the outer wheel, and which of the front wheel that is the outer one is determined by the sign of β_r. Four individual brake pressure requests are calculated. In the case of $\beta_r < 0$ the requested yaw moment will also be negative which makes the scalar P_{req} negative and its sign is therefore changed before it is requested to the front right wheel;

$$\begin{aligned} FL\_P_{req} &= \begin{cases} P_{req} & sign(\beta_r) \geq 0, \\ 0 & sign(\beta_r) < 0, \end{cases} \\ FR\_P_{req} &= \begin{cases} 0 & sign(\beta_r) \geq 0, \\ -P_{req} & sign(\beta_r) < 0, \end{cases} \\ RL\_P_{req} &= 0, \\ RR\_P_{req} &= 0. \end{aligned} \tag{3.5}$$

The pressure request is not passed on to the Brake Control Module (BCM) if the recorded actual β_r is smaller than a minimum value β_{min} or that the flag which toggles SSRA control on and off is set to 0. The tuning parameter β_{min} is needed because measurements and reference value is uncertain at small steering angles, i.e. corrections at straight line driving, why control requests should be neglected.

$$\begin{aligned} &if\ abs(\beta_r) \leq \beta_{r,min} \parallel SSRActrlon = 0 \\ &\quad FL\_P_{req} = FR\_P_{req} = RL\_P_{req} = RR\_P_{req} = 0 \end{aligned} \tag{3.6}$$

The output from the controller is then the four individual wheel brake pressure requests, and in the simulation environment this needs to be complemented with four flags indicating that we have a brake pressure request for the communication with the ESC model function. The resulting request is then sent to the BCM which is responsible for the actuation. If another actuation method of the correcting moment was chosen, for instance by rear wheel steering the constant G that transforms the yaw moment request would have to change in a suitable way, and in our case it changes with the current vehicle as part of the model based design.

4 Evaluation procedure

The major tool used for the controller model development has been a vehicle dynamics simulation tool called Vedyna 3.10 from Tesis Dynaware. Vedyna is implemented in the Matlab/Simulink environment which makes it possible to build Simulink models that interact with the model during simulation and afterwards post-process data in Matlab. The Vedyna vehicle model is modular and consists of the subsystems chassis, axles, individual axle steering, brakes, drive train, engine, transmisson and tires. Each subsystem can be replaced and the number of degrees of freedom can vary from eleven up to more then seventy depending on the respective vehicle and suspension type (Tesis DYNAware, 2006c). The developed controller has also been evaluated in vehicle tests.

4.1 Simulation vehicle model

The vehicle model used in the Vedyna simulations resembles a Volvo XC90. This vehicle model was chosen because an existing production like ESC was previously implemented in a XC90 Vedyna model. Other possible options for our choice of simulation model would have been to develop our own vehicle model and yaw rate based ESC function, but within the scope of the thesis work it would have been difficult to reach the same level of detail as with the Vedyna model. It is to a limited extent possible to alter parts of the Vedyna model, for instance by adding external brake systems and functions such as the ESC or an external tire model like the Magic Formula. Other parts of the model are hard to survey, as the functionality is implemented as S-functions which consists of pre-compiled blocks. This is a drawback as it makes the understanding of the Vedyna model more difficult.

The Volvo XC90 is a sports utility vehicle, SUV, which has a higher center of gravity than regular cars. This makes SUVs more susceptible to roll over, which is often handled by RSC functions that decrease the lateral force generation of the tires by increasing the longitudinal slip. The roll over stability would also be further increased by side slip angle control as the vehicle is most likely to roll over if it is sliding sideways, which then would be prevented by the side slip angle control.

In the XC90 Vedyna model the internal tire model has been replaced with the Magic Formula in a version called Delft-Tyre 1996. The tire data are collected from a Michelin Diamaris 235/60 R18 tire, which characteristics can be seen in Figures 2.3 and 2.5-2.6.

4.2 Test cases

As stated in Chapter 2, a vehicle equipped with a regular ESC system might not be able to detect a slow side slip build-up during cornering because the yaw rate threshold is not exceeded. This condition is being reproduced by the so called J-turn maneuver, in which the vehicle is cornering and the accelerator pedal is released. The maneuver is called a J-turn because the vehicle path resembles the letter J and the corresponding actual driving situation would be for instance a highway exit.

The second maneuver chosen for evaluation of the developed function is an obstacle avoidance maneuver, which is also referred to as a double lane change (DLC). This maneuver has been chosen because the controller's ability to limit the vehicle's side slip angle in the J-turn maneuver might impair the vehicles maneuverability in an emergency avoidance situation if not enough side slip is allowed. The purpose of this test case is not primarily to detect improvement of the vehicle's handling, but to ensure that the maneuverability is not made worse by the added SSRA control.

Table 4.1 below shows the expected outcome of the different control modes in the two maneuvers. Even if the stability in the J-turn maneuver would be significantly improved the controller model cannot be considered as acceptable if at the same time the maneuverability of the vehicle in the DLC is impaired.

Table 4.1 Test matrix showing the desired outcome of the SSRA Controller.

Driving scenario	Maneuver	Tested vehicle property	Without ESC	ESC	ESC + SSRA Ctrl
The bend at a motorway exit is tighter than you thought.	J-turn	Stability	**-**	**0**	**+**
An elk forces you to an evasive maneuver.	Double lane change, DLC	Maneuverability	**-**	**0**	**0/+**

In the vehicle simulation environment it is easy to perform tests that comprises of a series of specified inputs such as steering wheel angle and brake or accelerator pedal inputs. These tests are called open-loop maneuvers as the input to the vehicle is not depending on the resulting behavior. In other tests, such as the double lane change maneuver, the vehicle model tries to follow a specified path and therefore require closed-loop maneuver control in the simulation environment. This means that the input to the vehicle is depending on the current vehicles states. This is more difficult to achieve in the simulation environment, but is done in Vedyna using so-called driver models which use different control laws to reproduce human driving behavior (Tesis DYNAware, 2006a).

To evaluate the developed function one maneuver of each type has been chosen, the J-Turn maneuver which is an open-loop maneuver in the simulation environment and the double lane change that is a closed-loop maneuver where the driver model tries to get the vehicle through the advised path at as high speed as possible.

4.2.1 J-Turn

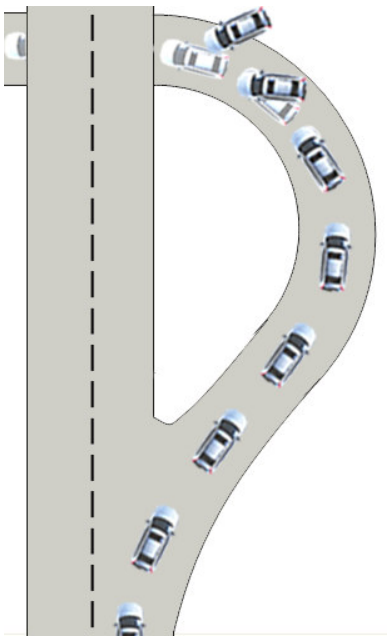

Figure 4.1 The J-Turn maneuver.

The J-Turn maneuver is based on an everyday driving scenario where the driver is leaving the highway. The cornering is done in too high speed and the tires are close to the adhesion limits but the driver is still in control of the vehicle. Suddenly, the driver realizes that he has misjudged the tightness of the curve and will not be able to stay on the road without speed reduction. The driver then lifts the accelerator pedal and by that gradually reduces speed but also generates a load transfer from the rear and to the front axle, see Figure 4.2.

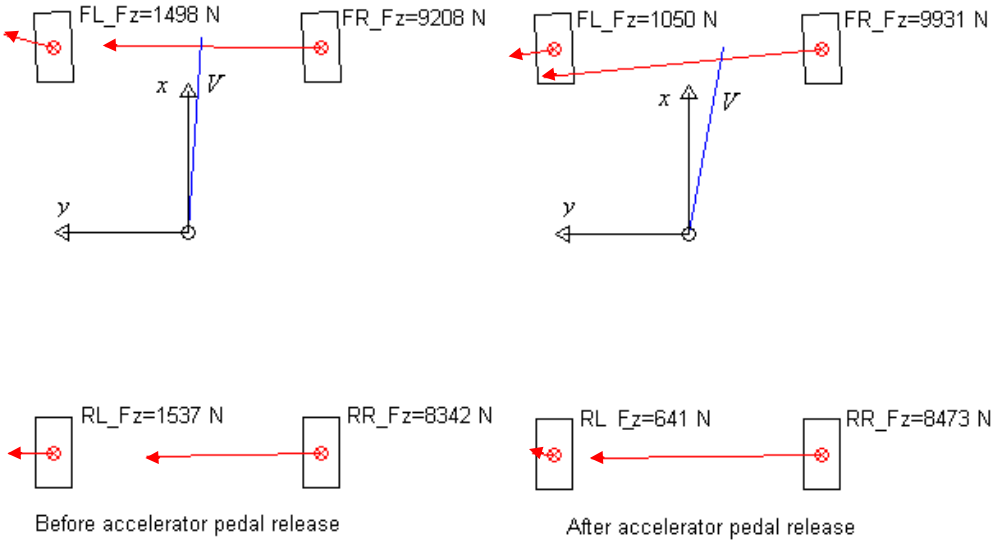

Figure 4.2 Force redistribution 1.61s after accelerator pedal release in a J-turn maneuver. The vectors with origin in the tire contact patches represent the tire forces in the horizontal plane and the vector in the CoG is the vehicle velocity. Forces FL_Fz –RR_Fz represent normal tire load on respective tire.

The load transfer has an effect on the tires ability to generate lateral forces. As seen in Figure 2.5 a larger normal load lead to a greater lateral force, provided that the slip angle stays the same, and vice versa. In this case it means that the front axle now is generating more yaw moment than the rear and the vehicle oversteers. This build up of the side slip angle may cause the driver to loose control over the situation and vehicle testing has shown that an ESC function may be insufficient in a J-Turn maneuver if the driver does not counter-steer. This maneuver should prove the need of side slip angle control since the yaw rate generated by the load transfer is relatively small and will not trigger the yaw rate based ESC.

Actual accidents resembling the J-turn maneuver have been described by for instance Sandin and Ljung (2007), who conducted an in-depth study of single vehicle crashes. The authors conclude that the most vulnerable vehicles for this type of accident is vehicles with a relatively high CoG compared with the vehicle wheel base, such as for instance compact cars or SUVs, as the load transfer is proportional to the center of gravity height.

Generating this maneuver in the Vedyna simulation environment is done in an open-loop structure where a sequence of inputs generates the desired maneuver.

Maneuver sequence

- Straightforward driving until desired speed V is reached.
- Ramp up a steering wheel angle SWA during t_r seconds starting at time t_{start}.
- Lift up accelerator pedal at time t_{lift}.

To further increase the effect of the accelerator pedal lift one can use the same approaches as the test driver's use, either to slightly increase the steering angle at the same time or give the brake pedal a light touch. However, this requires lot of iterations in the simulation environment to get the right timing for those inputs, and the vehicle is still more stable in the simulations than a real vehicle. This is a known problem, and as stated in Section 1.5 it is not part of the Master's Thesis to solve this issue. This problem is believed to be due to that the tire model does not represent the reduction in lateral force for high slip angles correctly, so that the vehicle have higher stabilizing forces in the simulation. As can be seen in the phase portrait figures in Chapter 2, the tire characteristics is very important for the stability of the vehicle and the real vehicle under the maneuver is more likely to resemble Figure 2.12 than the Vedyna simulation model.

To solve this issue one could manipulate the parameters in the Magic Tire formula to get a faster reduction of the lateral force at high slip angles. However, by utilizing a possibility in Vedyna called maneuver constraints, where the user can set different parameters such as the relative friction of each tire, the Magic formula can remain intact. To make the vehicle more susceptible to oversteer and thus more likely to perform the desired yaw, the relative friction of the rear wheels is reduced to 90%. The most relevant vehicle states and brake activity during a Vedyna simulation is presented in Figure 4.3.

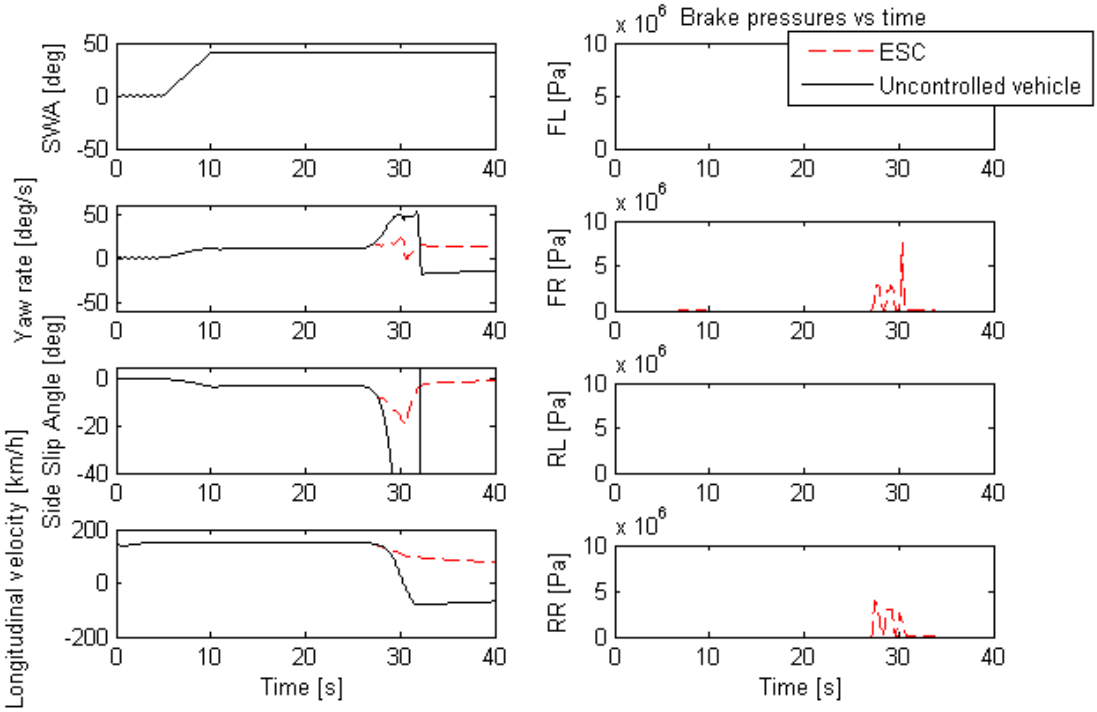

Figure 4.3 J-Turn on high μ surface with 90% relative rear axle friction. Inputs: V=150km/h, SWA=40°, t_r=5s, t_{start}=5s and t_{lift}=26s

In the test performed above the ESC controller does intervene but cannot manage to hold the side slip angle below 15 degrees which according to van Zanten (2002) is an upper limit for the average driver to still be able to handle the vehicle. This is due to the fact that when the tire lateral forces are saturated the vehicle becomes insensitive to changes in steering angle. Thus this limit is lower when the surface friction is reduced, i.e. on packed snow or on a wet surface. The ESC controlled vehicle in the figure above does not spin around completely as the uncontrolled vehicle does, but if the driver has lost maneuverability of the vehicle and started to skid sideways we consider it as if stability is lost.

4.2.2 Double lane change

There exists many different versions of double lane change maneuvers, for instance the ISO-DLC in which the width of the course is adjusted with respect to the tested vehicle. The maneuver studied here is a Consumer's Union double lane change maneuver. It is some times also referred to as the Consumer's Union Short Course test and it has been developed to test the maneuverability of a vehicle in an emergency situation. The test has been evaluated by NHTSA for rollover testing but is considered to be better suited for emergency handling than rollover stability (Forkenbrock et al., 2003). The test will be a good reference test for the developed function as it should improve emergency maneuverability at the best, and at least not make it worse than with only the regular ESC.

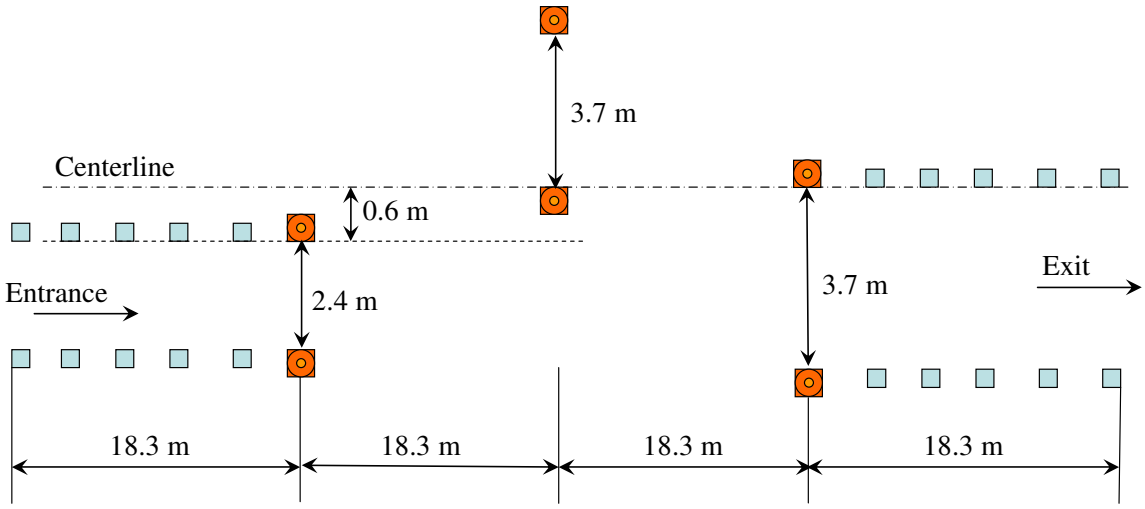

Figure 4.4 Consumer's Union double lane change setup.

Figure 4.4 shows the test setup of the Consumer's Union double lane change and the test should be performed as follows:

- The driver accelerates to the desired entrance speed as the vehicle passes the entrance cones the driver lets go of the accelerator and the brake pedal.
- The driver tries to steer the vehicle as fast as possible through the course, and the highest successful entrance velocity is recorded and compared with other similar vehicles.

A test is considered as successful if the vehicle passes through the intended course without hitting any cones.

As stated in Section 4.2 the double lane change is performed as a closed-loop control maneuver. The driver models in Vedyna are depending on two sets of input data, the first being target path settings such as course and speed and the second data set being driver parameters. The driver model tries to minimize deviations from the target path according to controller gains in the model. The driver model controller gains can be tuned to resemble a certain driving style, however such a classification has already been done for the Vedyna advanced driver model where it is possible to choose for instance a driver which is said to be "skilled_racy_smooth" or "untrained_careful_direct". An untrained driver model has a poor estimation of the vehicle states and is likely to push the vehicle outside of the adhesion limits and thereby loosing control of the vehicle, whereas a skilled driver has a good estimation and is therefore more likely to not exceed the limits of the vehicle. Racy or careful is a measure of the willingness to take risks, meaning that racy drivers can achieve higher accelerations and smooth or direct determines the response behavior of the driver. Lastly it is also possible to select a driver with or without preview, which means that the driver model is looking further ahead and is more likely to cut corners. This makes a driver model with preview unsuitable for our purpose as he will hit the cones at the entrance and exit of the double lane change maneuver (Tesis DYNAware, 2006a).

The ESC should give an untrained driver model the most help to manage an evasive maneuver, but the purpose here is to test one function against another, why the absolute increase in maximum maneuver speed with and without stability control function is not the most interesting parameter. To evaluate if the performance of the ESC system is impaired by the added SSRA control, the skilled_racy_smooth driver model has turned out to be more suitable as its steering input is smoother than that of an untrained driver model.

The target path for the double lane change is calculated by a Vedyna function which is optimized to calculate the path for an ISO-double lane change maneuver. The ISO-double lane change differs from the chosen Consumer's Union DLC as the ISO-maneuver is more drawn out and the distance in the second lane is longer. The Vedyna function is said to calculate the path efficiently as long as the proportions of the distances in the maneuver is kept, why it is considered to be usable also for the Consumer's Union DLC (Tesis DYNAware, 2006a). Furthermore, the driver model is not aiming at avoiding the cones, but to follow the specified trajectory, which makes the simulation somewhat different than a real vehicle test. Therefore, the maximum possible entrance speeds of the simulation might not be directly comparable to real vehicle tests, but it will give the possibility to evaluate ESC and ESC with added SSRA control relatively between different simulations.

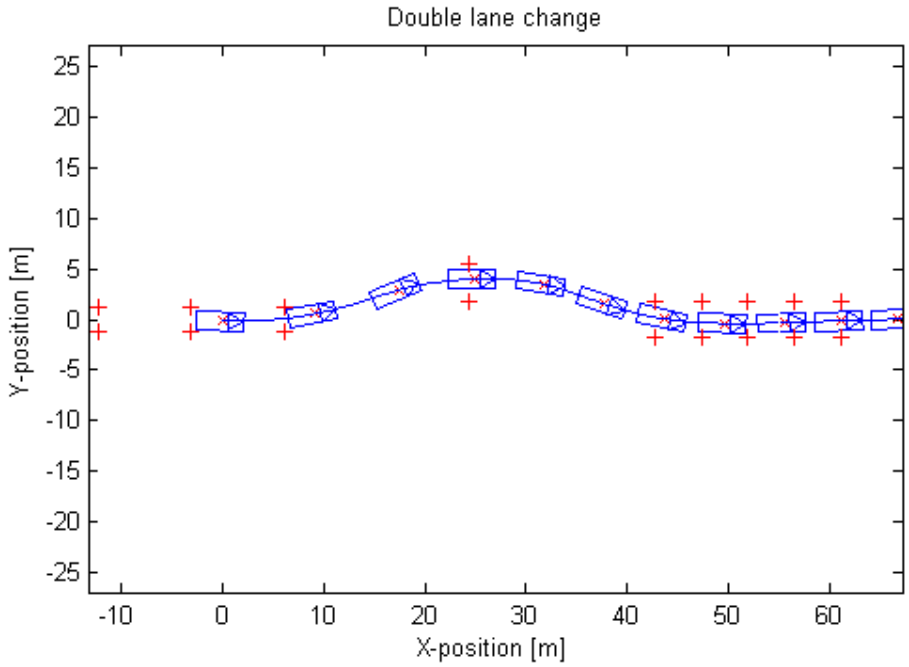

Figure 4.5 Vehicle trajectory for 66 km/h entrance speed with ESC.

Figure 4.5 shows the vehicle trajectory in the maneuver. The crosses represent the cones which should in real life occupy an area but here is reduced to points, and if the vehicle body can be detected outside of the cones the run is considered as a fail. The first three cones the simulation should in the real life test consist of 7 cones to make a longer entry strip. The entrance cones that can be seen in Figure 4.5 represent from where the entrance velocity should be measured. The exit strip should also be longer and consist of 7 cones, but it has been shown in the simulations that if the vehicle fails the test it does so before the last 2 cones and the driver model tries to follow the pre-determined trajectory anyway.

4.3 Vehicle testing

The car model used for evaluation of the SSRA controller in vehicle tests is a Volvo V70 T6 AWD of 2007 year's model. This vehicle differs from the Volvo XC90 used in the computer-based simulations but the use of another vehicle may demonstrate the gain of model based development. The test vehicle has four wheel drive and it is equipped with a yaw rate based ESC system. Brake pressure sensors are mounted on each of the four brake calipers, which make it possible to monitor the actual brake pressure at each wheel respectively. Furthermore, a connection to the Controller Area Network (CAN) bus has been installed, making it possible to communicate with the vehicle's electronic control units such as the Brake Control Module (BCM). The BCM is the part of the vehicle electronic control system that contains the ABS, TCS, and ESC functions and through it individual wheel brake pressure requests can be made.

4.3.1 Rapid control prototyping

The tight schedules in the automotive industry development processes have given birth to rapid control prototyping, which makes it possible to evaluate both the design and the implementation of new control algorithms in a fast and efficient way. If the developed controller is implemented in the Matlab/Simulink environment it is possible to download the model into a real-time hardware in an automated way by the use of the rapid control prototyping tool Dspace. The real time hardware platform, called Dspace MicroAutoBox, is capable to interact or bypass selected ECU functions. As the SSRA controller is developed and implemented as an addition to existing ESC systems, the BCM is kept active and the SSRA controller is interacting with the BCM by sending individual wheel brake pressure requests through a CAN-bus interface. Through the same CAN-bus connection a selection of the BCM signals is logged for post processing and monitoring during the tests. The BCM software in the test vehicle is equivalent to that of a production vehicle, with the exception of an added interface that allows external brake pressure requests and to toggle ABS, TCS and ESC on and off.

4.3.2 Test vehicle setup

The rapid control prototyping test setup consists of five units:

1. An OXTS RT3000 gyroscope with six degrees of freedom and GPS support used to measure the vehicle's motion.
2. A Dspace MicroAutoBox used to run the compiled controller model in real time.
3. A laptop with software capable of real time communication with the MicroAutoBox making it possible to tune our controller and log data.
4. A Data Acquisition System (DAS) that logs CAN-bus signals and the output from the brake pressure sensors.
5. A Volvo V70 where the BCM software is modified so that it can accept external brake pressure requests.

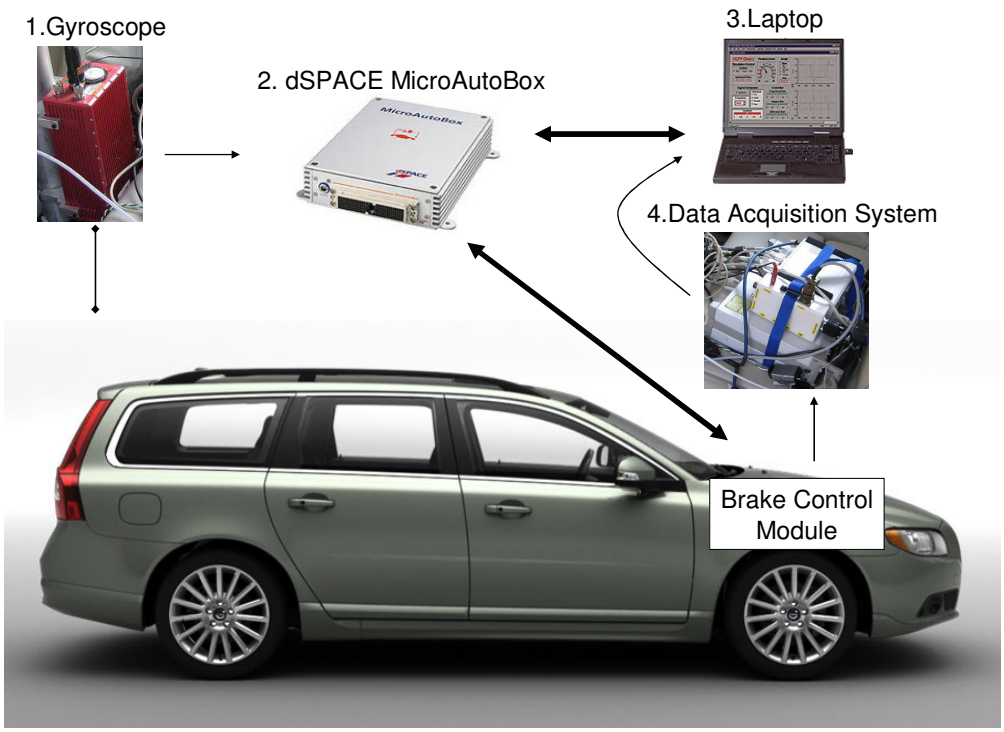

Figure 4.6 Rapid control prototyping setup. The bold arrows represent 2 way real time communication used for SSRA control of the vehicle.

The communication between the components in the rapid control prototyping setup is shown in Figure 4.6. The setup in the vehicle can also be seen in Appendix C where photos from the test day are attached. The gyroscope is installed between the driver and the passenger seat, just behind the armrest. It registers the vehicle body's motion in all the six degrees of freedom depicted in Figure 2.1. These signals are sent to the MicroAutoBox via a private CAN interface, where the signals are used by the SSRA controller model. The gyroscope signals is also relayed to the laptop where the measurements are logged for post processing.

The developed controller is running in the MicroAutoBox and acts by sending brake pressure requests to the BCM if a rear axle side slip error is recorded. The laptop is running a software program called Dspace Controldesk, which allows for real-time monitoring and tuning of the model currently running in the MicroAutoBox. The laptop is also used to log data from the gyroscope and the CAN-bus connected to the BCM. The data is transferred to the laptop through the MicroAutoBox which makes it possible to monitor it in real time using the Controldesk software.

In Controldesk two user interfaces was developed, one tuning interface where the control mode and the controllers tuning parameters could be altered and one monitor interface where the recorded sensor data could be monitored in real time and therefore quickly analyzed. The monitor interface can be seen in Figure 4.7.

Figure 4.7 The monitor and logging interface developed in Dspace ControlDesk.

In addition to the signals seen in the figure above the laptop also receives the brake pressure sensors output, a large amount of CAN-bus and internal BCM signals via the DAS. These signals are recorded by software belonging to the DAS and are only studied in the post-process procedure.

5 Results

5.1 Simulation results of the J-turn maneuver

The objective for the controller in the J-turn maneuver is to limit the vehicle side slip angle so that the driver remains in control of the vehicle. As is shown in Chapter 2 and in Figure 4.3 the vehicle can experience side slip angles large enough to endanger the driver's ability to control the vehicle even though it is equipped with a production like yaw rate based ESC.

Figure 5.1 below shows the resulting interventions when the SSRA controller is added to the production like ESC in the simulation model. The SSRA controller is tuned so that it intervenes in the maneuver when the accelerator pedal is released and the vehicle has started to build up a side slip angle.

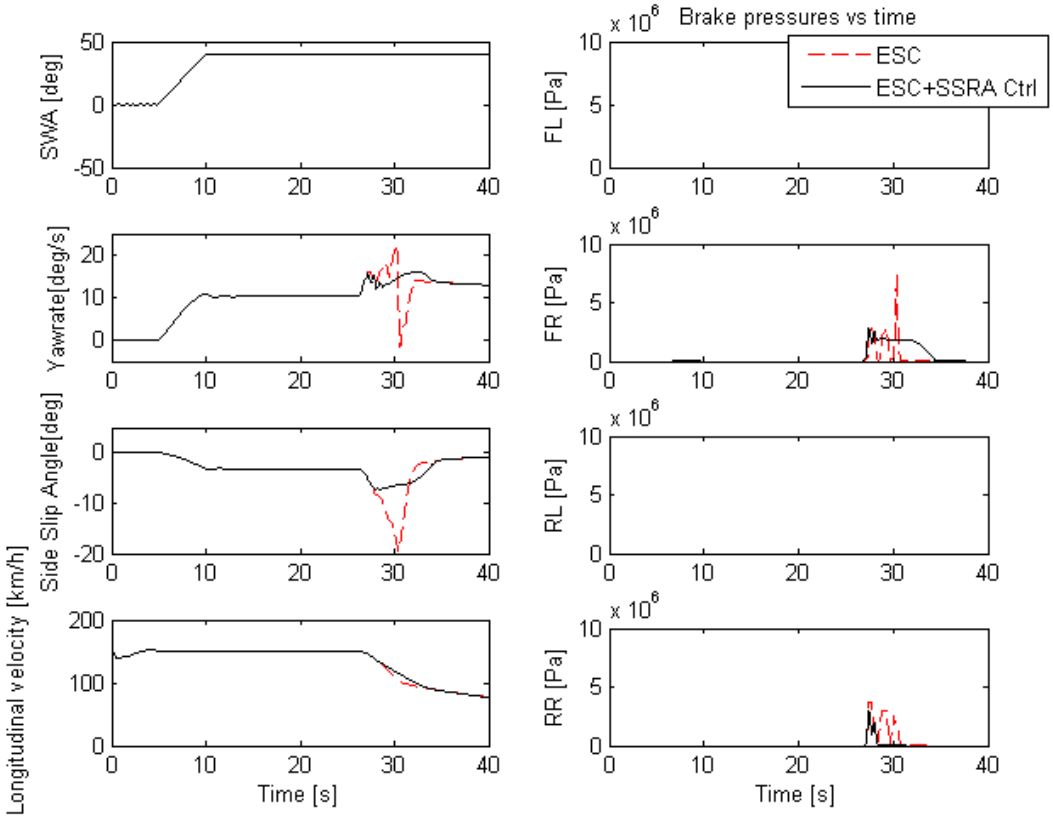

Figure 5.1 J-Turn on high μ surface with 90% relative rear axle friction. Maneuver parameters: V=150km/h, SWA=40°, t_r=5s, t_{start}=5s and t_{lift}=26s

The gain of the SSRA controller in the maneuver shown in Figure 5.1 is the added continuous braking on the front right wheel. Thanks to this intervention the vehicle side slip angle stays below eight degrees, which can be compared with the 20 degrees in the ESC case. Another benefit in the J-turn maneuver can be seen in Figure 5.2 below where the SSRA controller equipped vehicle does also manage to make a tighter turn despite the fact that the vehicle maintains a higher longitudinal velocity.

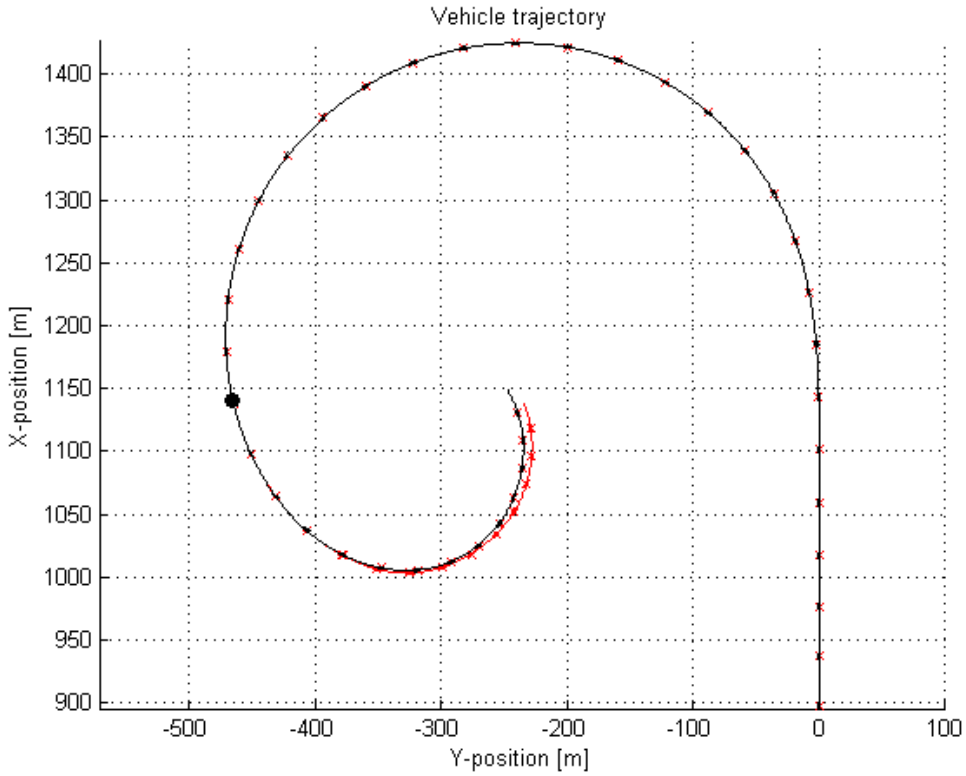

Figure 5.2 Difference in J-turn trajectories between ESC (outer trajectory) and added SSRA control (inner trajectory). Black round dot indicates accelerator pedal release, crosses represent 1 s time intervals.

If we use the previously described phase portraits of lateral velocity and yaw rate to evaluate the maneuver above we can easily see what difference the SSRA control does relative to the yaw rate based ESC interventions.

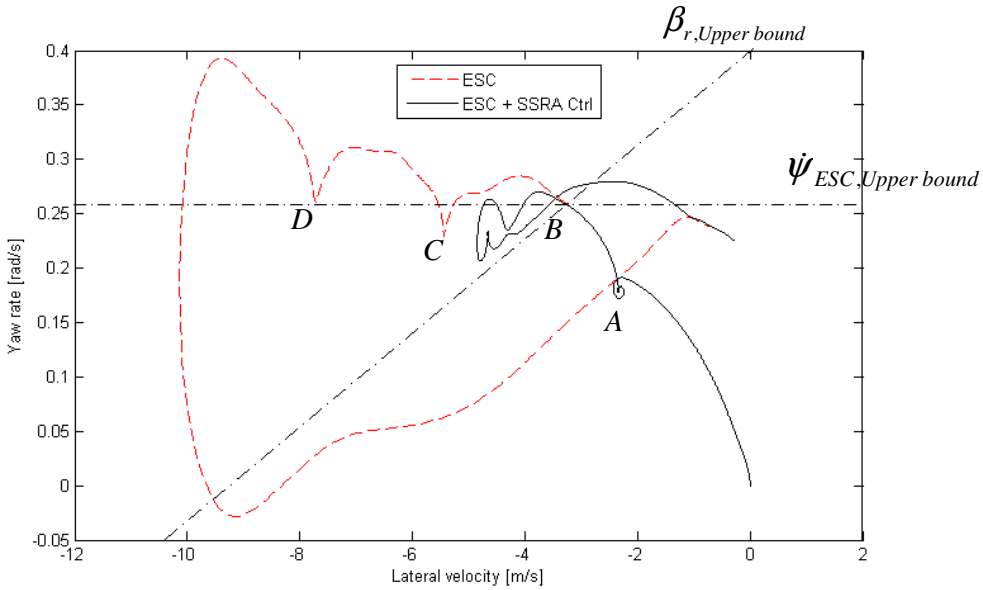

Figure 5.3 Vehicle states in the phase portrait for the two control modes. Point A represent steady state conditions before accelerator pedal release, Point B where interventions begin, Point C and D where ESC interventions ceases.

Figure 5.3 shows the difference between two runs, the dashed line with only ESC and the solid line with added SSRA control. The first thing that happens in the maneuver is that the vehicle enters a steady state condition (A) and when the accelerator pedal is released the vehicle experiences an increase in both lateral speed and yaw rate. The SSRA controller reacts when the rear axle side slip exceeds the SSRA upper bound (B). This upper limit is generated by the reference model for the given maneuver. The SSRA controller reference model is tuned so that it allows more side slip than the vehicle has in the previous steady state condition, and this can be considered as a margin (the distance between A and B) that prevents unwanted actuation. Thanks to the continuous braking on the front right wheel the SSRA controller manages to limit the side slip angle as seen in Figure 5.1.

The ESC also reacts in point B with a brake pulse on the front right wheel as its yaw rate error threshold is exceeded, which results in the yaw rate dip to point C. When the yaw rate now is below the ESC threshold, the intervention ceases. The next intervention that pushes the yaw rate to point D is done with a higher yaw rate reference value as the vehicle now has started to slow down. Therefore, the ESC yaw rate threshold is larger than the horizontal line depicted in Figure 5.3, which only is valid for the initial conditions in point A.

The conclusion from studying the phase portrait of the different control modes is that the SSRA controller is working as intended with improved interventions in oversteering situations such as the J-turn maneuver.

5.2 Simulation results of the double lane change

The purpose of the double lane change maneuver is to act as a reference maneuver in which the vehicle's maneuverability is maintained with the added rear axle side slip control. If the rear axle side slip control function is to aggressively tuned this might not be the case, as it can make the vehicle heavily understeer by not allowing any side slip at all.

The results from the simulations with the added rear axle side slip control shows that the vehicle can manage the specified Consumer's Union DLC at an entrance speed of 68 km/h, compared to the vehicle with only the ESC which can manage 66 km/h. The difference between the interventions in the two cases can be seen in Figure 5.4 below.

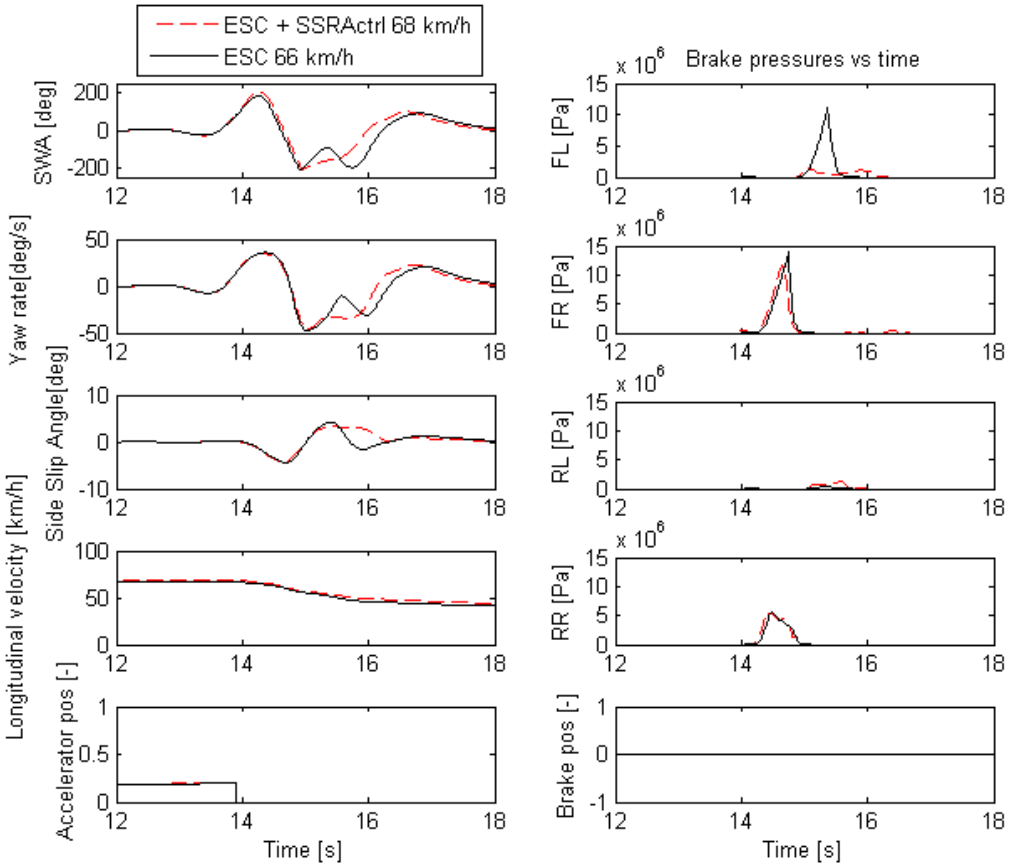

Figure 5.4 Difference between original ESC and added SSRA control in Consumer's Union DLC. SSRA control increases maximum entrance speed because of earlier intervention on FR wheel.

The reason that the vehicle with the added SSRA control can manage 2 km/h higher entrance speed is likely because of the earlier intervention on the front right wheel as seen in Figure 5.4. This gives a larger effect of the intervention and the driver can keep the steering wheel angle more smoothly without having to counter-steer and finally it results in a much smaller and more drawn-out braking on the front left wheel.

From the simulations performed it cannot be concluded that the SSRA control will enhance the performance in the Consumer's Union DLC as the ESC is likely to be tunable for an earlier intervention like the one seen in Figure 5.4 above, but it clearly shows that the SSRA controller with the current tuning does not impair the vehicle's emergency maneuverability.

5.3 Vehicle test results

The vehicle tests were carried out using the same basic maneuvers as for the simulations. Two test drivers with different experience level carried out the tests, with Driver no. 1 being the most experienced and responsible for the major part of the test driving. This driver carried out 21 successful runs and Driver no. 2 carried out four J-turn maneuvers in different control modes. The intention of the test driving was to evaluate the same kind of control modes as in the simulations, with uncontrolled and ESC controlled vehicle as reference and then ESC and SSRA control for verification of the developed function. However, a fourth test mode had to be considered as the interaction between ESC and SSRA control was not entirely successful. The onboard ESC system did not fully allow SSRA control brake pressure requests when the two systems were running at the same time, probably because the SSRA pressure request to the BCM is considered as a driver braking request which can be overridden by the ESC if it is considered to have an undesired effect. To solve this, the ESC was shut of and only ABS kept active to prevent wheel locking in the maneuvers in the SSRA Control mode where the vehicle was only stabilized with the SSRA controller. Table 5.1 shows the successfully completed tests.

Table 5.1 Performed vehicle tests.

Test no.	Driver no.	Maneuver	Speed [km/h]	Control Mode
1	1	Steady state right turn	50	ESC
2	1	Steady state left turn	50	ESC
3	1	J-turn	100	Uncontrolled
4	1	J-turn	100	ESC
5	1	J-turn	100	ESC
6	1	J-turn	100	ESC
7	1	J-turn	100	ESC
8	1	J-turn	100	ESC
9	1	J-turn	100	ESC + SSRA control
10	1	J-turn	100	ESC + SSRA control
11	1	J-turn	100	ESC + SSRA control
12	1	J-turn	115	ESC + SSRA control
13	1	J-turn	120	ESC + SSRA control
14	1	J-turn	100	SSRA control
15	1	J-turn	100	SSRA control
16	1	DLC without cones	100	ESC
17	1	DLC without cones	100	ESC + SSRA control
18	1	DLC Volvo test	90	ESC
19	1	DLC Volvo test	95	ESC + SSRA control
20	1	DLC Volvo test	90	SSRA control
21	1	DLC Volvo test	90	SSRA control
22	2	J-turn	100	ESC
23	2	J-turn	100	SSRA control
24	2	J-turn	100	ESC + SSRA control
25	2	J-turn	100	SSRA control

Test no. 1 and 2 were performed to compute the actual cornering stiffness of the test vehicle, to be able to compare parameters carried over from a simulation model. The calculated cornering stiffness from the measurements was not considered to be of the correct magnitude, and therefore the values from the simulation model of the V70 were kept. This decision was taken as the reference model followed the vehicle satisfactory with the simulation model parameters, however it was tuned so that the stiffness distribution changed from front to rear with 5 %, making the reference model more understeer. This tuning of the reference model decreased the upper bound seen in Figure 5.3 of the allowed rear axle side slip. How the actual measured vehicle states and the reference model coincide can be seen in Figure 5.9, where it is clear from the plot of the yaw rate that our model nonetheless is more oversteer than the actual vehicle. Even further tuning of the model with more stiffness to the rear axle could make the SSRA controller act more aggressively to deviations in rear axle side slip.

The steady state turns in Test no.1 and 2 also show a problem that was experienced early during the testing, the gyroscope was not perfectly aligned in the vehicle and thus picked up small amounts of longitudinal speed in the lateral direction during straight line driving. At about 28 m/s (100 km/h) longitudinal speed the lateral speed sensor picked up about 1 m/s although the vehicle was traveling straight forward. The effect of the misalignment can be seen in Figure 5.5 of the velocities in the two steady state runs.

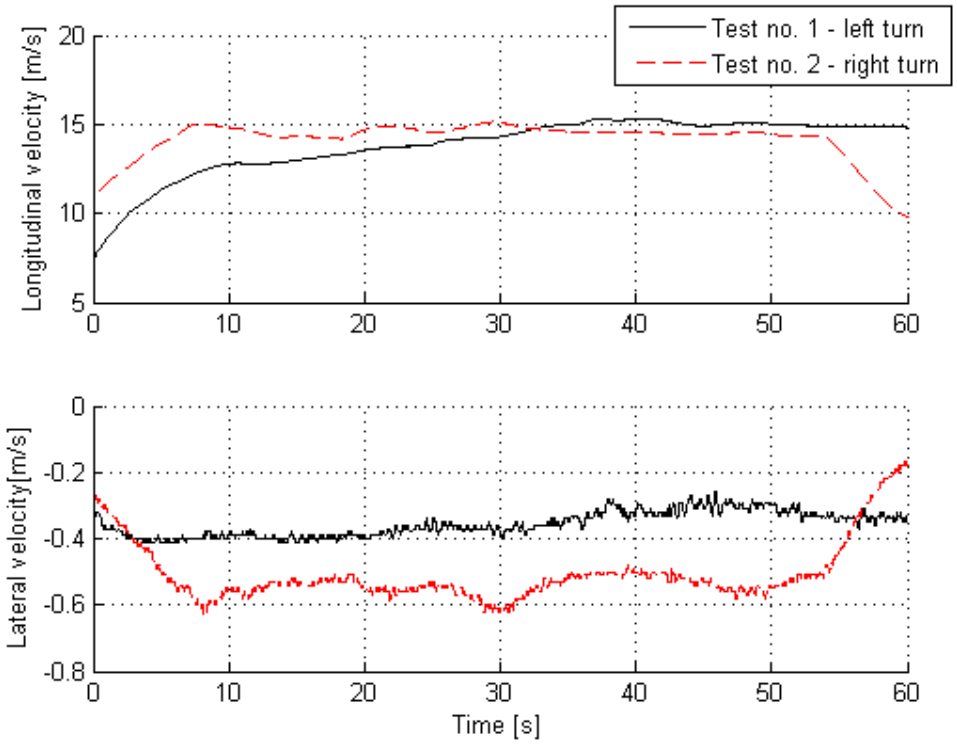

Figure 5.5 Lateral and longitudinal velocities measurements from the RT3000 gyroscope in 47 m radius steady state corner.

Figure 5.5 shows the offset in the lateral velocity as both recorded velocities are negative for the opposite turning directions. The difference of 0.2 m/s between the two test runs should be centered around the x-axis, which means we have an offset of about 0.45 m/s at the given longitudinal speed. This introduced a new problem to the controller model that was not

experienced in the simulations. If traveling straight at 100 km/h the measured lateral speed would be about 3.6 km/h and this would indicate a side slip angle of about 2 °. To prevent the controller to intervene because of this a switch that disabled the controller below measured lateral velocities of 1 m/s was implemented in the rapid prototyping model, and this proved to be efficient as the lateral velocities in the considered maneuvers was well above this value. The lateral velocity measurements also seemed to improve in accuracy when a higher lateral velocity was picked up in an actual maneuver.

5.3.1 J-turn test results

As can be seen in Table 5.1 eleven successful J-turn maneuvers were performed by Driver no. 1 and four by Driver no. 2. The maneuver was carried out slightly different between the two drivers why the results between the two is not directly comparable, but the more experienced Driver no. 1 had very good repeatability in the steering wheel input and entrance speed of the maneuver. Figures 5.6 and 5.7 show the driver input steering wheel angle and the entrance velocity of Tests 4-8.

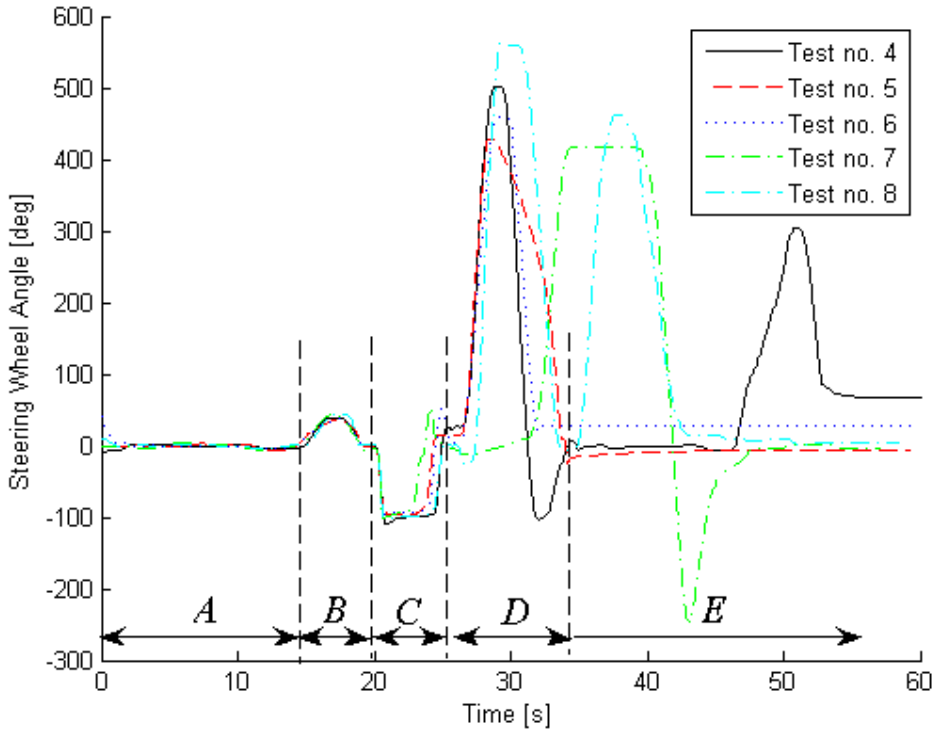

Figure 5.6 Steering wheel angle for J-turn maneuver tests with only ESC active. Rapid steering input at 20 s (section C) shows the beginning of the maneuver, and at the same time the accelerator pedal is released.

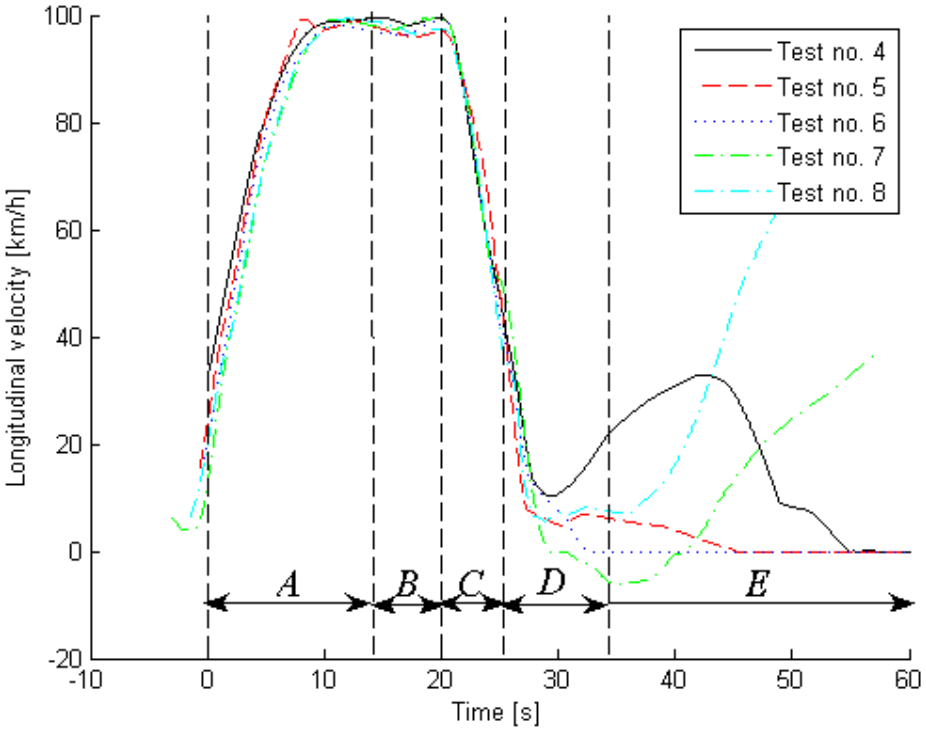

Figure 5.7 Longitudinal velocity during J-turn maneuver, entrance speed for all five tests are slightly below 100 km/h. Sections shown corresponds to the ones in Figure 5.6.

In Figure 5.6 the beginning of the J-turn maneuver can be seen as a dip in SWA at 20 s (between section B and C), the positive steering input before in section B is the driver positioning the vehicle on the test surface so that the maneuver can be performed without entering the barrier surrounding the test area. The large SWA inputs after the maneuver in section D is the test driver counter-steering to keep the vehicle on the test track. The plots in Figures 5.6-5.8 have been shifted in time so that the steering wheel is turned at the same time for all five maneuvers, and as can be seen in Figure 5.6 and 5.7 the entry speed and steering wheel input are very similar in between the tests. Section A represents the acceleration phase before the maneuver, and section E contains measurements that have been done after the maneuver has been completed.

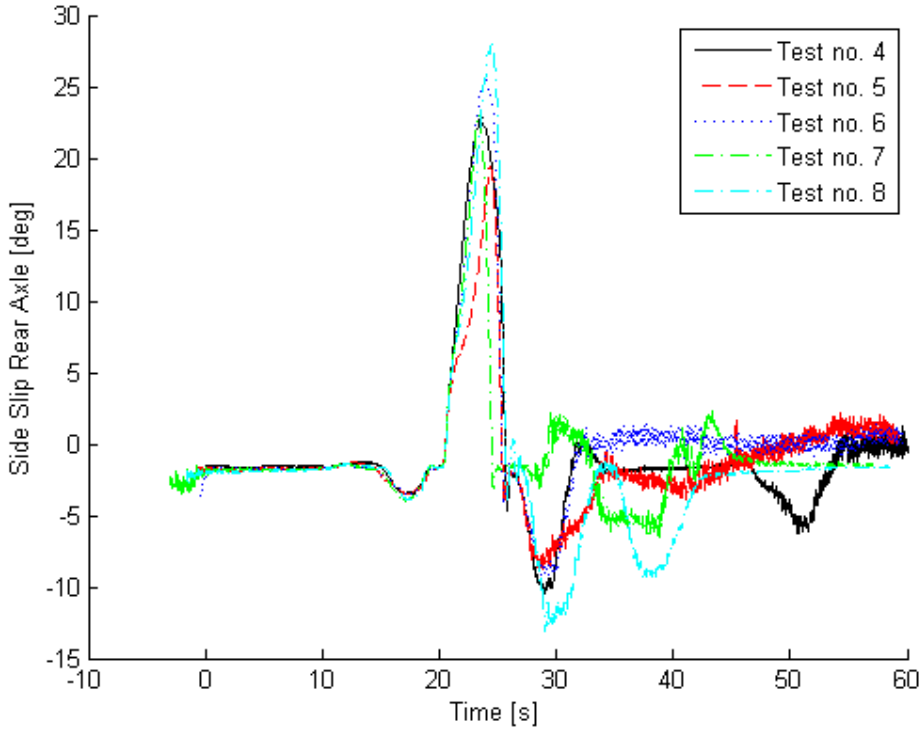

Figure 5.8 Rear axle side slip for the different Tests no. 4-8.

Figure 5.8 above shows the rear axle side slip for five different test runs with only the ESC active, and the maximum of the SSRA ranges from 19 to 28° in the current tests. If one examines the SSRA plot compared to the SWA for the same maneuvers it seems that the reason to why the vehicle does not reach even higher side slip angles is that the test driver has started to abort the maneuver and steer in the opposite direction before the SSRA has its peak in 4 out of 5 tests. This indicates that if the SWA would be kept at 90 ° as in the simulations, the vehicle would become totally uncontrollable for a normal driver even though the ESC is active as both front and rear axles would be far beyond their saturation limits. Plots of SWA and SSRA for test 4-8 can be seen in Appendix C, Figures C1-5.

Analogously to the previous Figures 5.5 – 5.8, Test no. 9-11 with both SSRA control and ESC shows SSRA in the same range and the same behavior, although Test no. 9 which has the smallest maximum SSRA indicates that the request from the SSRA controller in this case was let through, but not in Test no. 10 and 11. The brake request and the BCM estimate of the brake pressures for Test no. 9 can be seen in Figure 5.9 below, and figures corresponding to those of Test no. 4-8 above can be found in Appendix C, Figures C8-10 for Test no. 9-11.

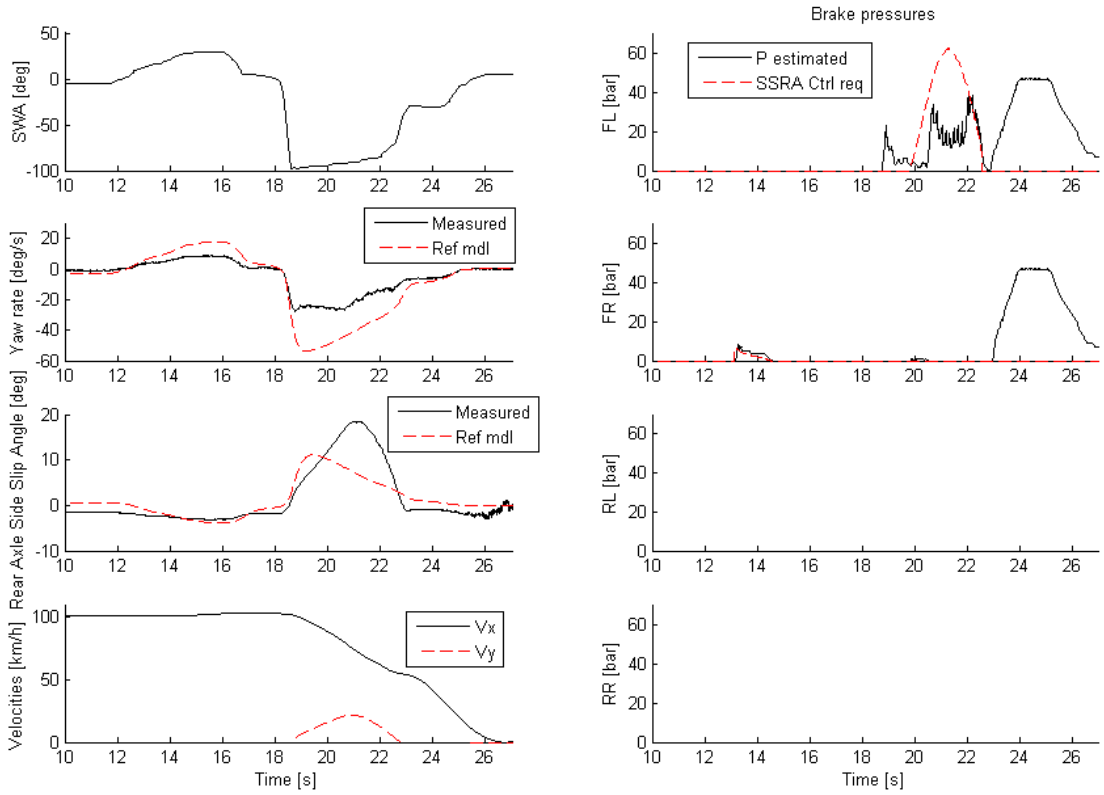

Figure 5.9 Vehicle states and brake pressures for Test no. 9. Notice the upper right figure with FL brake pressure, where the requested pressure from our controller is the dashed line and the solid line is the pressure estimate from the BCM.

Two successful tests were performed with only the SSRA controller active, where the SWA and entrance speed in the maneuver were comparable to that of Test 4-8. Figure 5.10 shows the vehicle states and brake pressures from Test no. 15, in which the side slip at the rear axle was limited to 17°. The upper right plot shows the brake pressures on the front left wheel, where the dashed line represents the requested brake pressure from the SSRA controller, the solid line the estimated pressure calculated by the BCM and the dash-dot line the actual pressure at the wheel which was measured with pressure sensors.

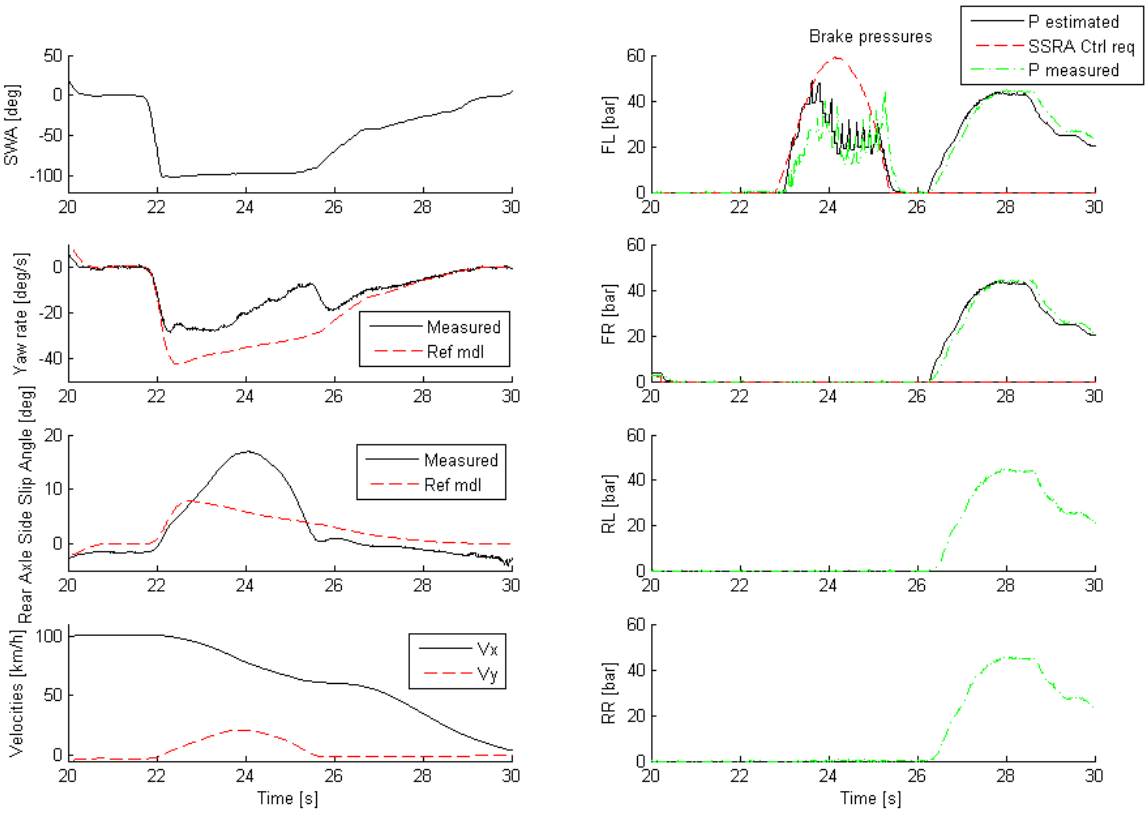

Figure 5.10 Brake pressures (BCM estimate and measured values) and vehicle states for the J-turn in Test no. 15, with only SSRA control active. Note the difference between estimated and measured brake pressure at each wheel.

It is interesting to note that the SSRA has its peak before the driver starts to return the steering wheel in contrast to Test no. 4-8 with only the ESC active. This means that the decrease in SSRA is mainly due to the added yaw moment induced by the brake pressure on front left wheel. It also indicates that an addition of SSRA or SSA control to a normal ESC system would make it less dependant on the driver to make the correct decision and counter-steer in a stressful situation, which is the case for Test no. 5-8. When only the ESC is active it does not make enough counter measures until the driver starts to counter-steer because even though the side slip angle is growing, the yaw rate is fairly close to the reference value. For comparison between the two control modes Figure 5.11 below shows the SWA and SSRA for the two Tests no. 15 and no. 6.

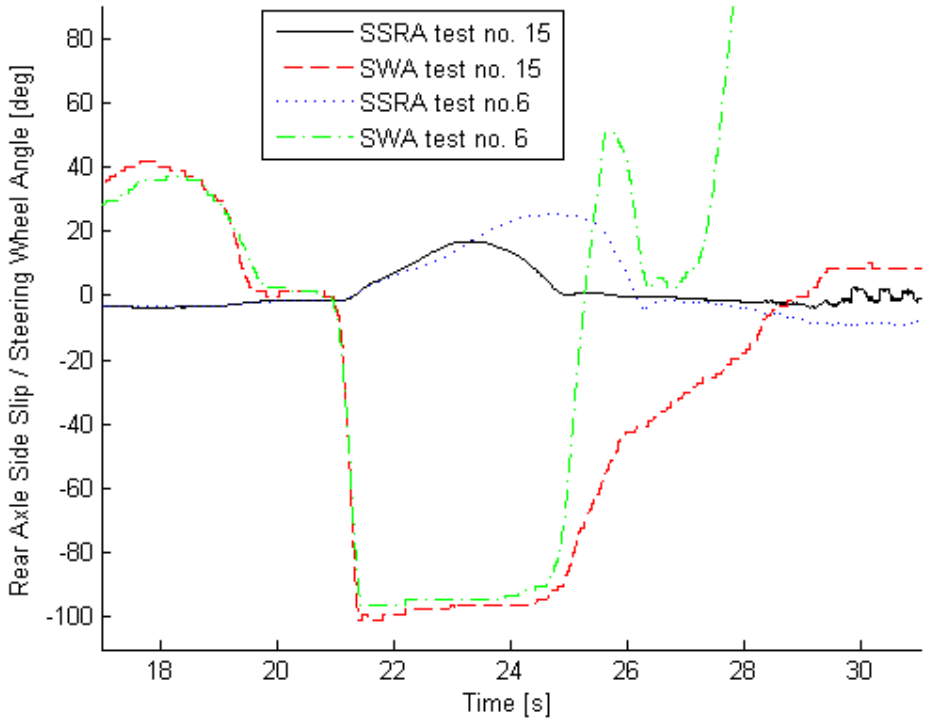

Figure 5.11 SSRA and SWA for Test no. 6 and no. 15. Notice that SSRA control counteracts the SSRA build up before driver starts to counter-steer, whereas ESC does not recognize any significant yaw rate error before.

In the tests no. 14 and 15 the maximum of the SSRA is 15° and 17°, whereas in Tests 4-8 the average is 24° why it can be concluded that the added SSRA control is beneficial. This was also the perception of Driver no. 1 (Bohlin). One thing to be noted is that Driver 2 (Jacobson) who has tested similar systems said that he was expecting a more powerful intervention from the SSRA control. This could perhaps be achieved if the BCM interface was working as desired, with the SSRA controller being able to work together with the ESC system, and thus also be able to achieve higher slip values than what was possible to reach in the current ABS mode. As ESC had to be turned off in the BCM and only the ABS was kept active only ABS values of longitudinal slip was possible to achieve, which means that the brake pressures were limited so that the longitudinal slip was kept around 10-20 %. If the BCM would have allowed brake pressure requests in ESC mode, deeper slip up to approximately 50 % would have been achievable, which would decrease the lateral force generated by the outer front tire and thus more efficiently counteract the oversteering.

The most important conclusion from the analysis above is perhaps that adding SSRA control makes the ESC system less dependant on the driver as it can intervene against the SSA build up without relying on the driver to start counter-steering.

5.3.2 Double lane change test results

Unfortunately it was not possible to perform the same DLC maneuver in the vehicle tests as in the simulations. The reason for this is that it was not possible to find the marked position for the Consumer's Union DLC on the test track. As time was limited two DLC like maneuvers without cones were performed (Test no. 16 -17) by Driver no. 1, to be able to get some data to evaluate from a DLC like maneuver with the SSRA controller. Later it was possible to perform four more DLC tests with cones, which increased the repeatability but the positioning of the cones were not based on a standard test but on a setup used by VCC for testing of their ESC systems.

Test no. 18 and 19 are the most interesting DLC tests as they show how SSRA control can affect the performance in a DLC maneuver. It has been our concern that a too aggressive tuning of the SSRA controller might impair the vehicle's maneuverability in an evasive maneuver such as the DLC, as it can make the vehicle too heavily understeered. From the simulations it was concluded that an earlier intervention added by the SSRA control was beneficial in the DLC maneuver. The major difference between the Consumer's Union DLC and the maneuver performed in the Tests 18-21 is that the distance in the second lane is longer in the vehicle tests. In this kind of test the vehicle is likely to keep building up side slip angle when the vehicle has entered the second lane to go straight for a short distance. Analogously to the J-turn maneuver, the yaw rate based ESC does not detect this as its yaw rate does not increase enough to exceed the allowed upper limit. In Test no. 18 only ESC was allowed to intervene, and the resulting brake pressures and vehicle states can be seen in Figure 5.12 below.

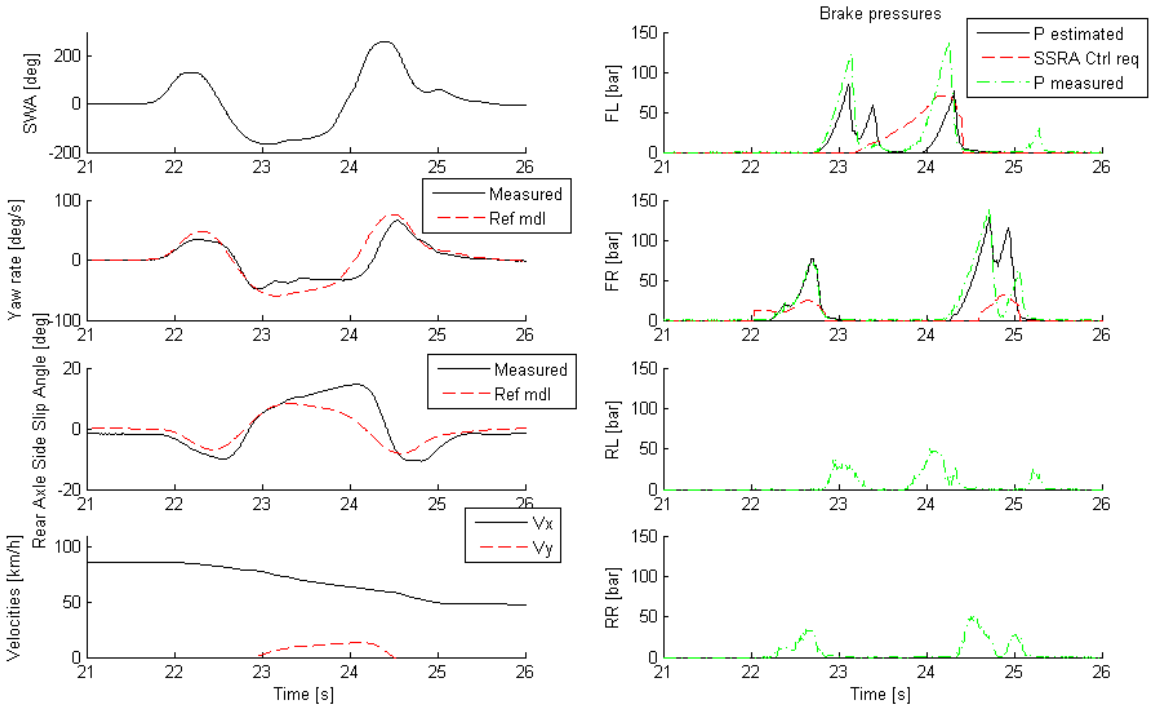

Figure 5.12 Vehicle states and brake pressures for Test no. 18 during a double lane change with only ESC active. SSRA Ctrl req shows what pressure SSRA control would request if allowed to intervene.

As can be seen in Figure 5.12, the front left wheel experiences two oversteering intervention brake pulses, with the accompanying brake pressures on the rear left wheel as described in Chapter 1.3. The dashed line represents the pressure the SSRA controller would introduce if allowed to, which is due to the error in SSRA also seen in the figure. In the following Test no.19 ESC and the SSRA controller was active at the same time, and this time the SSRA controller succeeded with its brake pressure request, as seen in Figure 5.13 below.

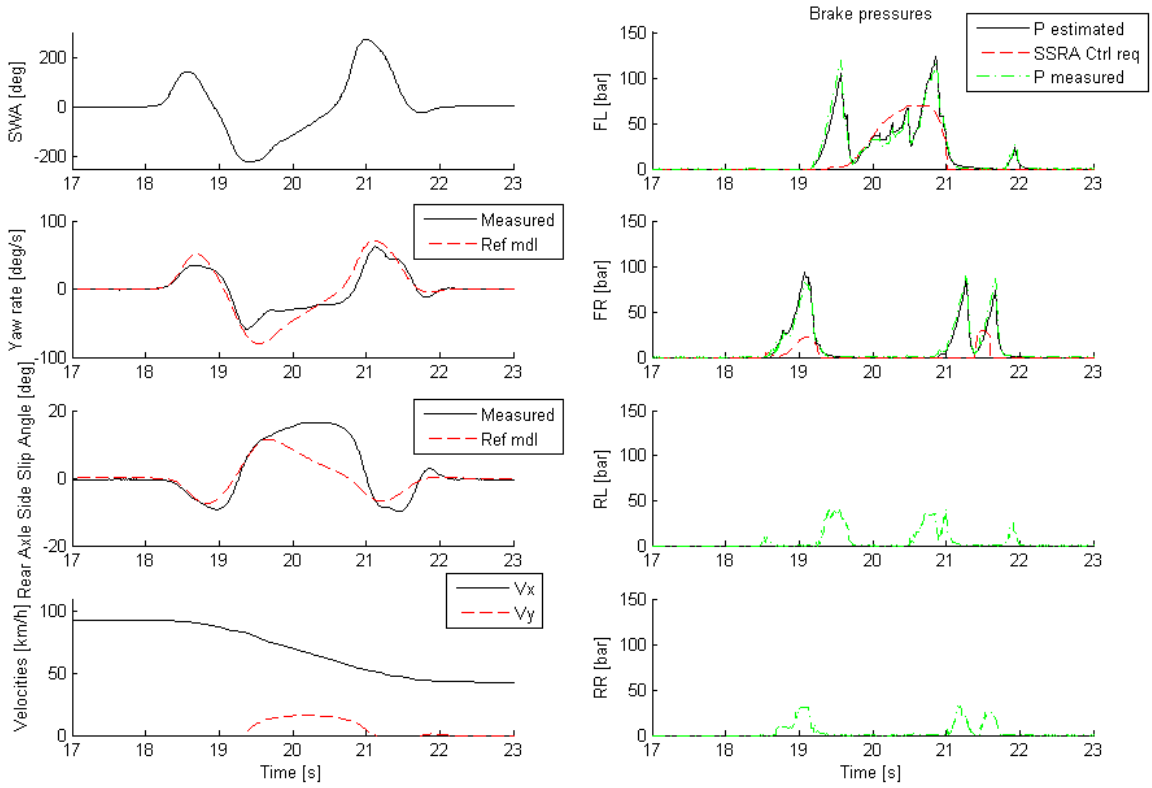

Figure 5.13 Vehicle states and brake pressures for Test no. 19 during a double lane change with both ESC and SSRA control active.

The major difference between the two tests is that the entrance speed in Test no. 19 was 95 km/h compared to 90 km/h in Test no. 18 which would make the test more difficult for the driver. Test Driver no. 1 which performed the DLC tests found the added intervention seen in the top right plot in Test no. 19 seen in Figure 5.13 to be helpful. In this test the SSRA controller succeeds with its brake pressure request and thus helps the driver to slow down the build up of the side slip angle, which goes unnoticed by the regular ESC. This shows that SSRA control also has the potential to increase the performance of a vehicle in evasive maneuvers, as this difference also was indicated and experienced by our test driver in the two cases where the DLC maneuver was performed without the cones. The two Tests no. 20 and 21 which were carried out with only the SSRA control active were not efficiently compared to the ESC. The reason to this is that the function only brakes the front wheels and also is intended as just an add-on to the existing ESC.

5.4 Model based development results

The model based controller described in Chapter 3 calculates a correcting yaw moment. By calculating the moment instead of the required brake pressures directly it enables us to implement different actuation systems or braking strategies if needed.

The model based approach showed itself successful in the vehicle tests as it was possible to use the same controller model as used in simulations although a different car model was used. The vehicle tests were installed and performed successfully in less than 12 hours. This would not have been possible if the tuning of the controller parameters would have been more extensive.

The only tuning parameter that had to change in between the simulation environment and the vehicle tests was the tuning of the cornering stiffness values, which was likely to be depending on the uncertain cornering stiffness values for the V70 taken from a Vedyna model. A part from the cornering stiffness, the minimum side slip intervention limit had to be increase to approximately 2° because of the offset in lateral velocity in the gyroscope sensor signals.

6 Conclusion

The introduction of Electronic Stability Control systems has been very successful in reducing accidents, but there is still a potential to further improve their ability to help the driver both by increasing stability and maneuverability of the vehicle. The result of the Master's Thesis shows that adding rear axle side slip control to existing ESC systems can improve the vehicle stability in oversteering situations such as in the J-turn maneuver. This is done for two reasons; the first being that the vehicle no longer can build up a side slip angle at a slow rate and the second that the vehicle stability control system can intervene in this situation without being dependant on the driver to make the correct decision to counter-steer in a critical situation. Furthermore, it has been shown that adding this functionality to the ESC does not necessarily impair the vehicle maneuverability in evasive maneuvers, but instead has a potential to improve the performance with up to 2 km/h higher entrance speed.

The simulations have been helpful in the development process of the controller, as it has been possible to easily make changes and analyze their effects. Thanks to the model based development approach of the controller it was successfully moved from the XC 90 simulation model to a rapid prototyping V70 vehicle model. The only changes that was made in the model between the two different setups was a change in model parameters and some slight tuning of the reference models cornering stiffness values.

The vehicle tests were enabled by the approach that was chosen for the thesis, where the SSRA controller was developed as an additional function to existing ESC systems. The tests confirmed the simulation results and also gave valuable feedback from the test drivers.

Given the positive results of rear axle side slip control it seems that benefits could be expected if the measurement and estimation of side slip and rear axle side slip angle could be solved in a reliable and efficient way. In a larger perspective SSRA control can be part of improving active vehicle safety even further and thereby help to reduce the number of fatalities in car accidents.

6.1 Further work

In Chapter 5 the vehicle test results indicated that the vehicle could be even further stabilized in the J-turn maneuver if larger longitudinal slip values were allowed during intervention from the SSRA controller. This could be a subject to investigate for further work, and one would then implement a slip request interface between the SSRA controller and the BCM unit.

All the tests and simulations carried out in the Master's Thesis has been performed on high friction surfaces, and therefore no limiting of the reference model with respect to the currently available friction has been necessary. To enable the controller to do appropriate interventions during low friction conditions, it could be necessary to alter the reference models cornering stiffness depending on an estimation of the friction. Otherwise, the upper limit of the allowed SSRA is likely to be too high compared with the slip angle limit where the tires become saturated.

Lastly, vehicle testing indicated that in the more drawn out double lane change maneuver benefits could be made from SSRA control when the vehicle entered the second lane, why it could also be of interest to study a single lane change maneuver.

References

Abe, M., Kano, Y., Suzuki, K., Shibahata, Y., & Furukawa, Y., (2001), *Side-slip control to stabilize vehicle lateral motion by direct yaw moment*, JSAE Review 22 (2001) p 413–419

Andreasson, J., (2007), *On generic Road Vehicle Motion Modelling and Control*, Diss. Royal Institute of Technology, Stockholm, Sweden

Bauer, H., (1999), *Driving-safety systems,* Stuttgart, Germany: Robert Bosch GmbH

Chumsamutr, R., Takehiko, F., Abe, M., (2006), *Sensitivity analysis of side-slip angle observer based on a tire model*, Vehicle System Dynamics Vol. 44, No. 7, July 2006, p 513–527

Dang J.N., (2004), *Preliminary results analyzing the effectiveness of electronic stability control (ESC) systems*, Washington D.C., USA. National Highway Traffic Safety Administration.

European Road Safety Observatory, (2006a), *Annual statistical report 2006*, http://www.erso.eu/safetynet/fixed/WP1/2006/SN_1_3_ASR_2006_final.pdf, Accessed 2007-08-16

European Road Safety Observatory, (2006b), *Traffic safety basic facts 2006– Main Figures*, http://ec.europa.eu/transport/roadsafety_library/care/doc/safetynet/2006/bfs2006_sn-kfv-1-3-mainFigures.pdf, Accessed 2007-08-08

Evans, L., (1998), *Antilock brake systems and risk of different types of crashes in traffic,* The 16th International Technical Conference on the Enhanced Safety of Vehicles (ESV) Proceedings, June 1998; Windsor, Canada. p. 445-461

Forkenbrock, G.J., Garrot, W.R., Heitz, M. & O'harra, B.C., (2003), *An Experimental Examination of Double Lane Change Maneuvers That May Induce On-Road, Untripped, Light Vehicle Rollover,* SAE International, Warrendale, PA, USA

Fukada, Y., (1999), *Slip-Angle Estimation for Vehicle Stability Control*, Vehicle System Dynamics, Vol. 32, No. 4, p 375-388

Guillermo, B., Nilsson, H., (2006) *Vehicle Stability Control for Roadside Departure Incidents by Steering Wheel Torque Superposition – Developed for and Evaluated in the Chalmers Driving Simulator*, Msc. Thesis, Department of Applied Mechanics, Chalmers University of Technology, Gothenburg, Sweden, p 1, Figure 2 from www.autoliv.com

Håbring, F., (2006), *Active rear wheel steer systems analysis – an actuator requirements approach*, Msc Thesis. Department of Applied Mechanics, Chalmers University of Technology, Gothenburg, Sweden

Kiencke, U., Nielsen, L., (2000), *Automotive Control Systems*, Berlin, Germany: Springer-Verlag

Lie, A., Tingvall, C., Krafft, M. & Kullgren, A., (2005), *The effectiveness of ESC (Electronic stability control) in reducing real life crashes and injuries*, 19th International Technical Conference on the Enhanced Safety of Vehicles Conference (ESV), 6-9 June 2005; Washington D.C., USA. Paper No 05-0135

Nagai, M., (2007), *The perspective of research for enhancing active safety based on advanced control technology,* Vehicle System Dynamics, Vol. 45, No. 5, May 2007, p 413-431

Pacejka, H.B., (2002), *Tyre and Vehicle Dynamics,* Delft, Netherlands. Elsevier Butterworth-Heinemann

Piyabongkarn, D., Rajamani, R., Grogg, J.A., Lew, J.Y., (2006). *Development and Experimental Evaluation of A Slip Angle Estimator for Vehicle Stablility Control*, Proceedings of the 2006 American Control Conference; 14-16 June 2006; Minnesota, USA. p. 5366-5371.

Sandin, J., Ljung, M., (2007) *Understanding the causation of single-vehicle crashes: a methodology for in-depth on-scene multidisciplinary case studies*, Int. J. Vehicle Safety, Vol. 2, No. 3, pp.316–333.

SIS, (1994), *ISO 8855 – Road Vehicles – Vehicle dynamics and road-holding ability – Vocabulary*, SIS, Stockholm, Sweden

SAE International, (1976), *SAE J670e - Vehicle Dynamics Terminology, Recommended Practice*, SAE International, Warrendale, PA, USA

TESIS DYNAware, Technische Simulation Dynamischer Systeme GmbH (2006a). *veDYNA 3.10 Driver Manual*. Munich, Germany

TESIS DYNAware, Technische Simulation Dynamischer Systeme GmbH (2006b). *veDYNA 3.10 Standard Data Requirements*, Munich, Germany

TESIS DYNAware, Technische Simulation Dynamischer Systeme GmbH (2006c). *veDYNA Product Catalogue*, Munich, Germany

Wong, J.Y., (2001), *Theory of ground vehicles – Third edition*, New York, USA: John Wiley & Sons

van Zanten, A.T., (2000), *Bosch ESP Systems: 5 Years of Experience,* SAE International, Warrendale, PA, USA

van Zanten, A.T., (2002), *Evolution of Electronic Control Systems for Improving the Vehicle Dynamic Behavior*, Stuttgart, Germany: Robert Bosch GmbH

Personal Communication

Andreas Bohlin, Volvo Car Corporation, 2007-10-03

Bengt Jacobsson, Volvo Car Corporation, 2007-10-03

Appendix A – Simulink controller model

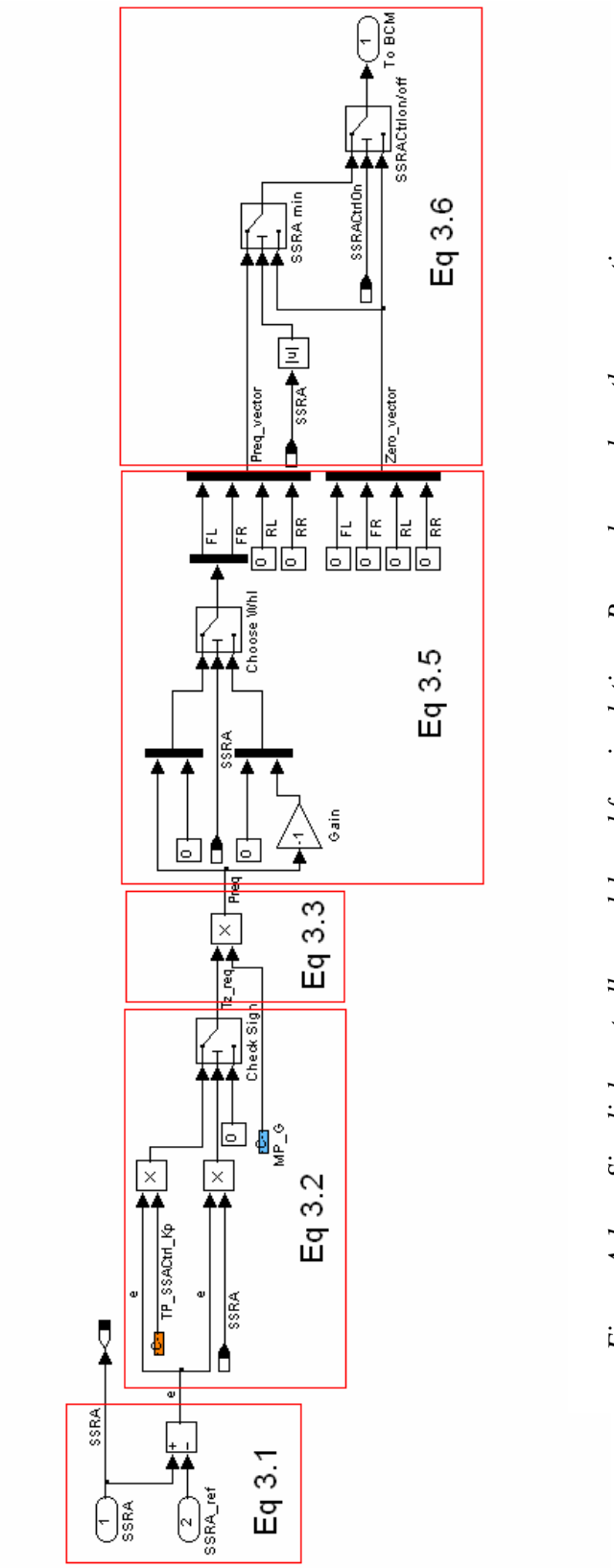

Figure A.1 Simulink controller model used for simulations. Boxes shows where the respective equations in Chapter 3 is implemented. In the simulations and vehicle testing a gain, K_p, of approximately 21000 Nm/rad (375 Nm/°) has been used.

Appendix B – Pictures of vehicle test setup

Figure B.1 OXTS RT3000 Gyroscope mounted between roof and floor and Data Acquisition System placement in the back seat of the test vehicle.

Figure B.2 Dspace MicroAutoBox running controller model placed in the luggage compartment of the test vehicle.

Figure B.3 Jonas Östh with laptop running control and logging software in the test vehicle.

Appendix C – Vehicle test data plots

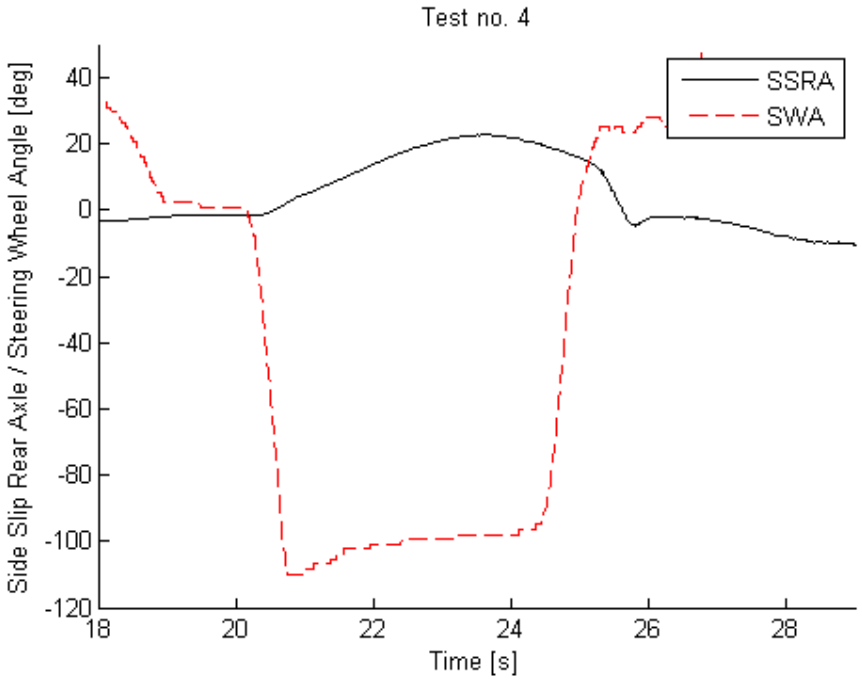

Figure C.1 SWA and SSRA for test drive no. 4. SSRA has peaked before SWA is returned to and the maneuver is aborted. This indicates that ESC handles the situation.

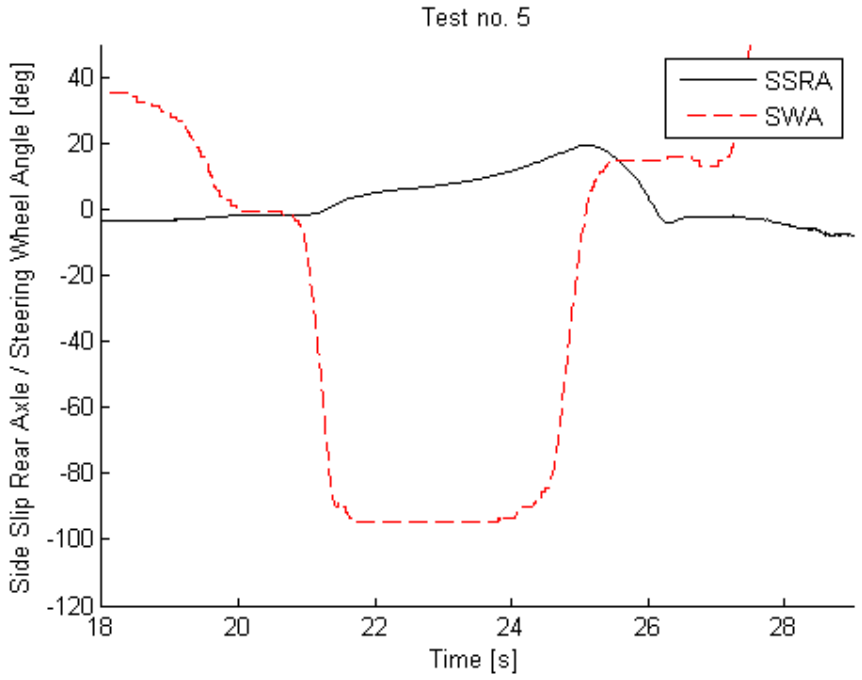

Figure C.2 SWA and SSRA for test drive no. 5. SSRA has not yet peaked before SWA is returned and maneuver aborted, this indicates that the vehicle would spin if the driver had not aborted the maneuver.

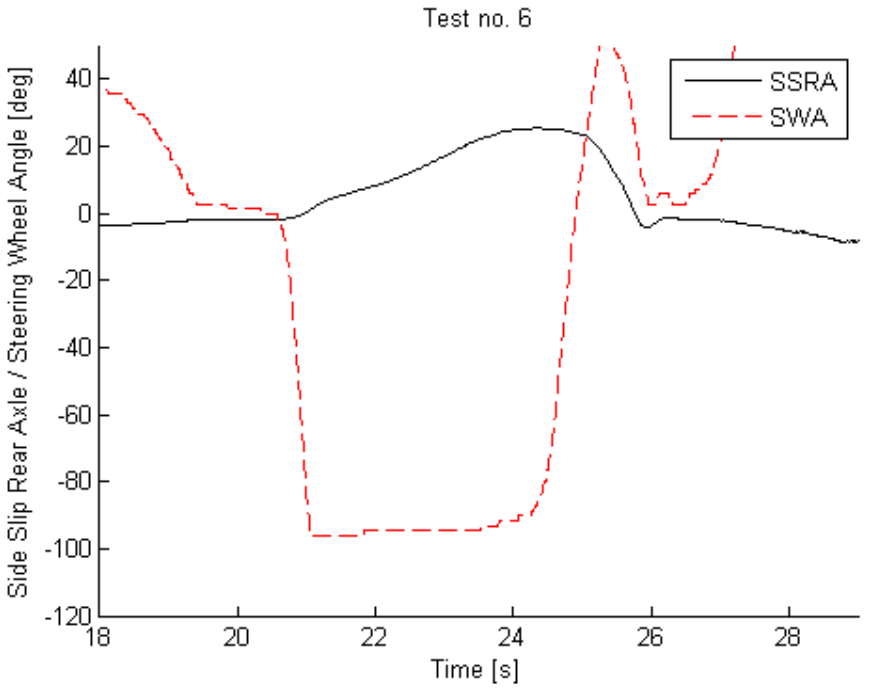

Figure C.3 SWA and SSRA for test drive no. 6. As in Figure B2 SSRA peaks before SWA is returned.

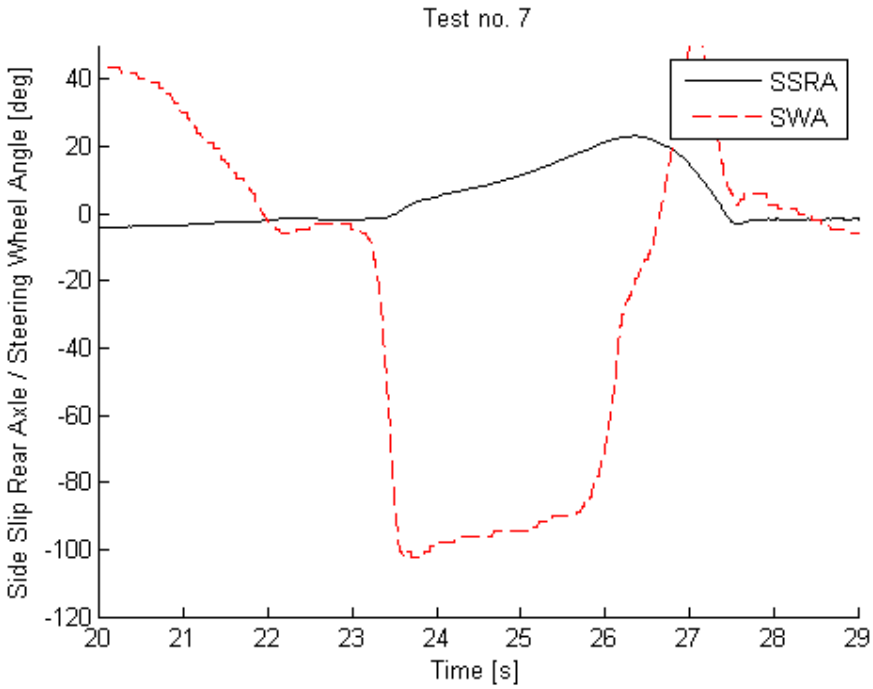

Figure C.4 SWA and SSRA for test drive no. 7. Same as previous figures.

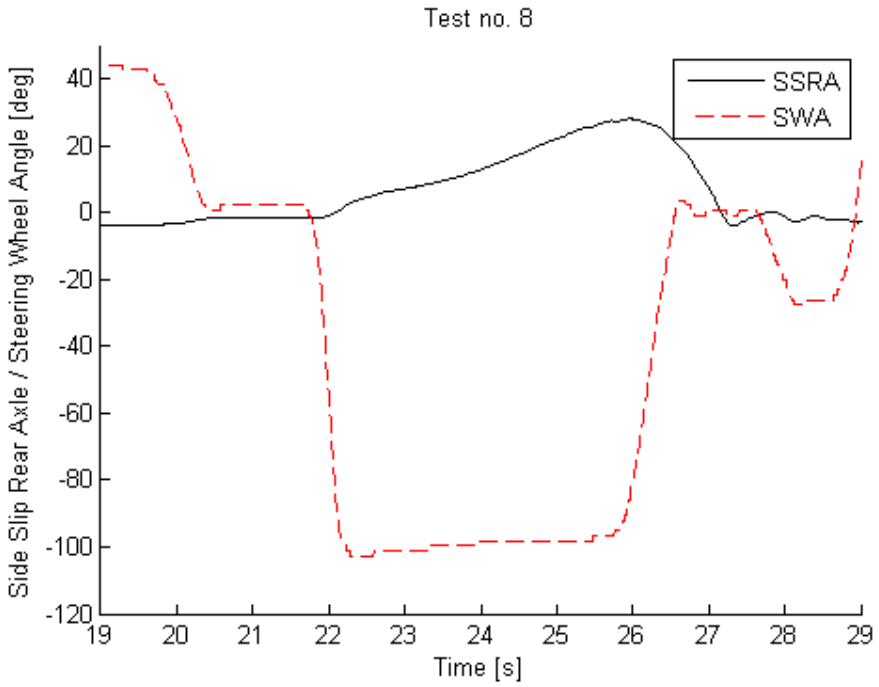

Figure C.5 SWA and SSRA for test drive no. 8. Same as previous figures.

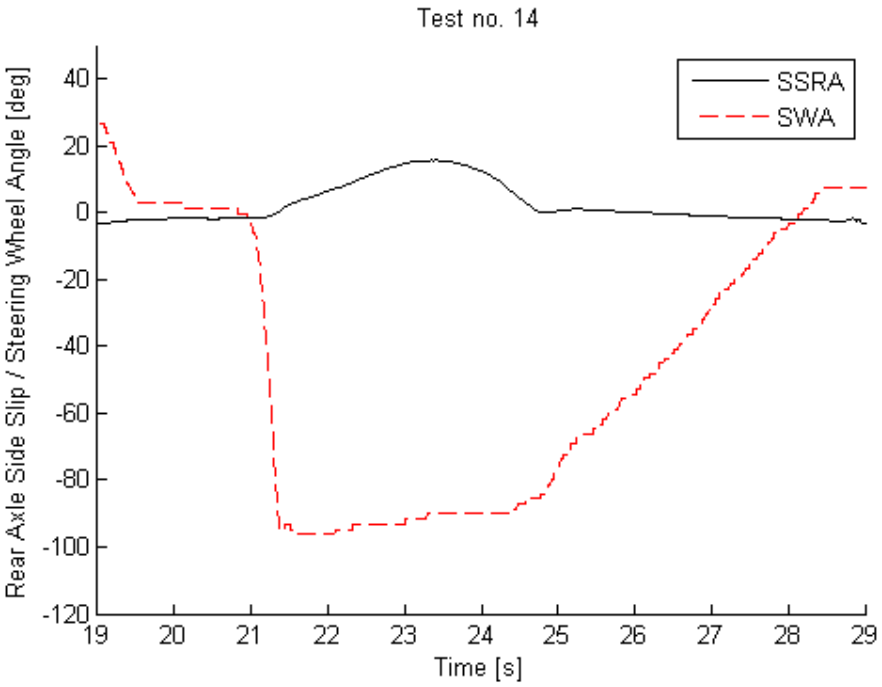

Figure C.6 SWA and SSRA for test drive no. 14. SSRA has peaked and is decreasing before maneuver ends because of SSRA control.

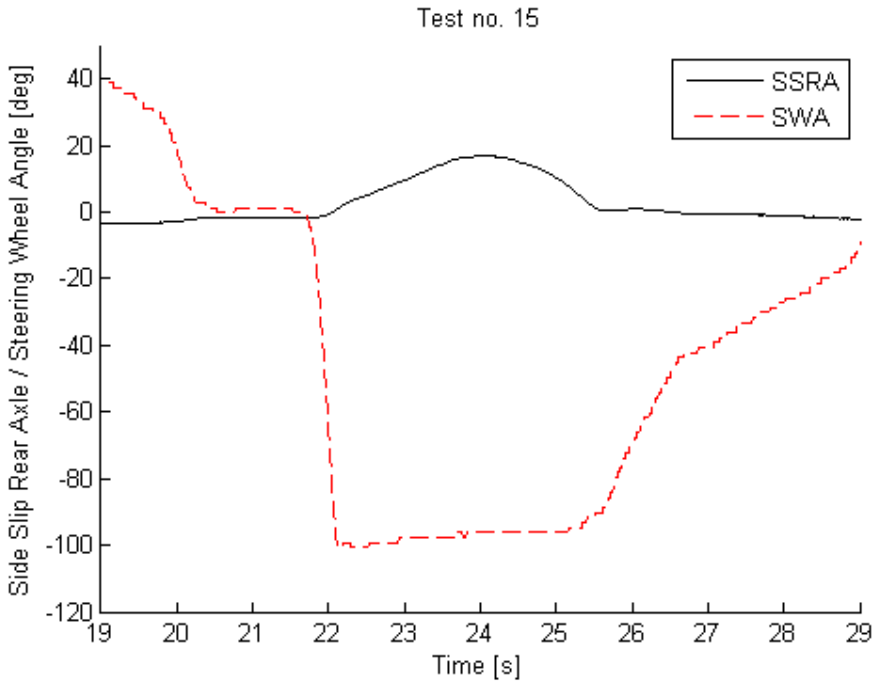

Figure C.7 SWA and SSRA for test drive no. 15. SSRA has peaked and is decreasing before maneuver ends because of SSRA control.

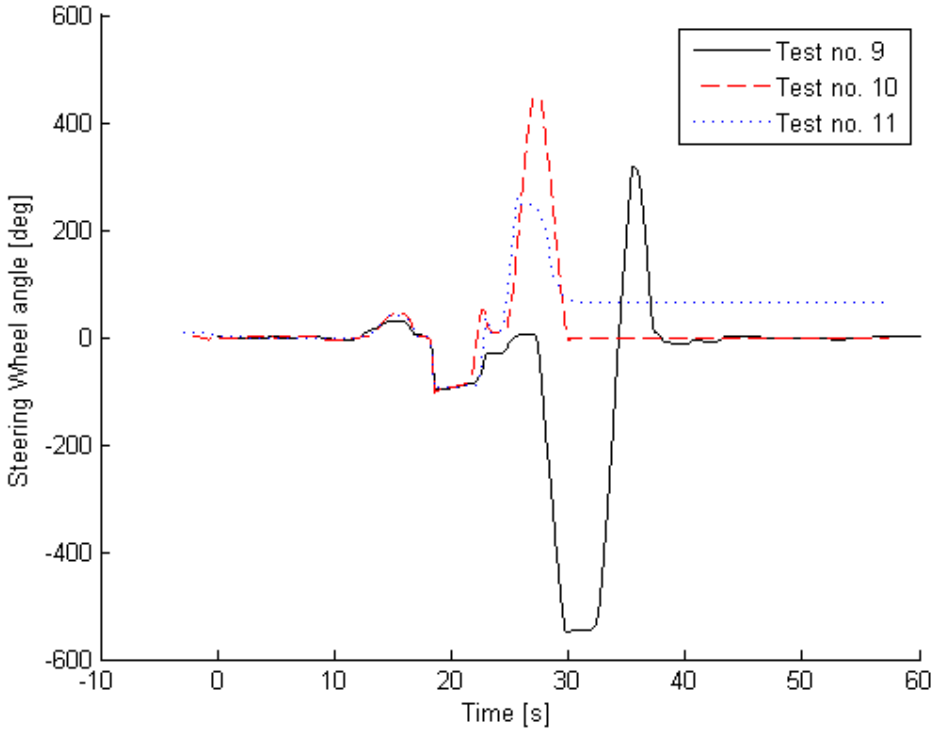

Figure C.8 SWA for test no. 9 – 11, ESC with added SSRA control.

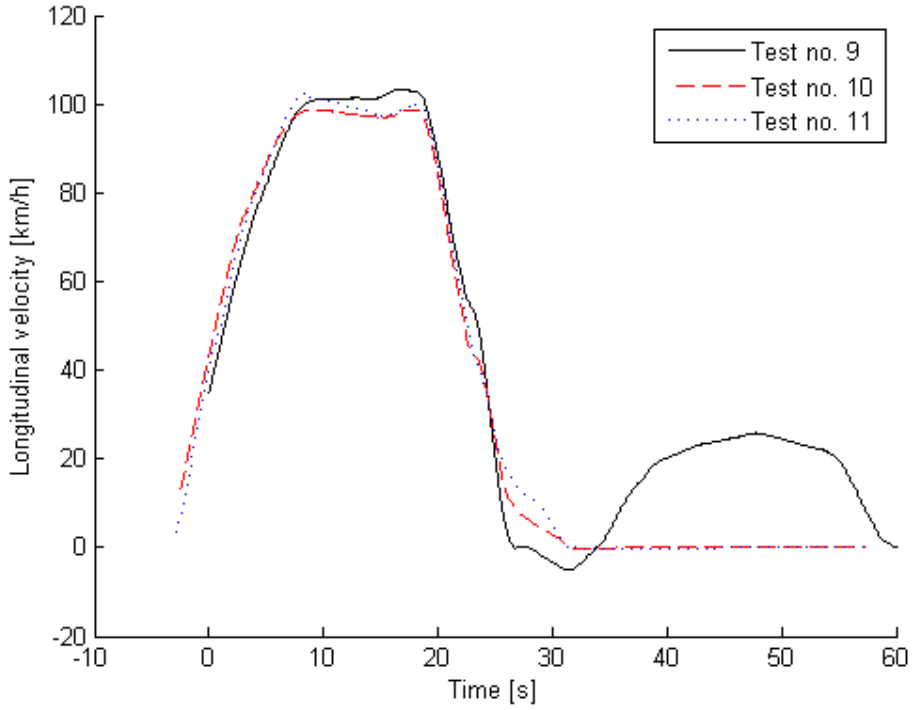

Figure C.9 Longitudinal speed for test no. 9 – 11, ESC with added SSRA control.

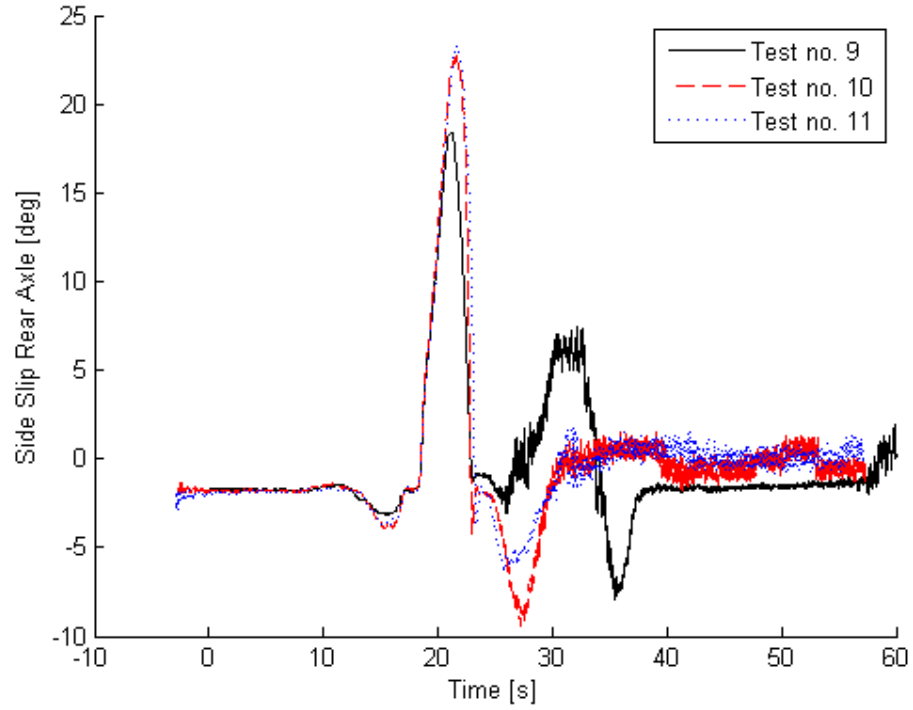

Figure C.10 SSRA for test no. 9 – 11, ESC with added SSRA control. In test 9 the SSRA controller succeeded in the pressure request, hence the reduced SSRA.

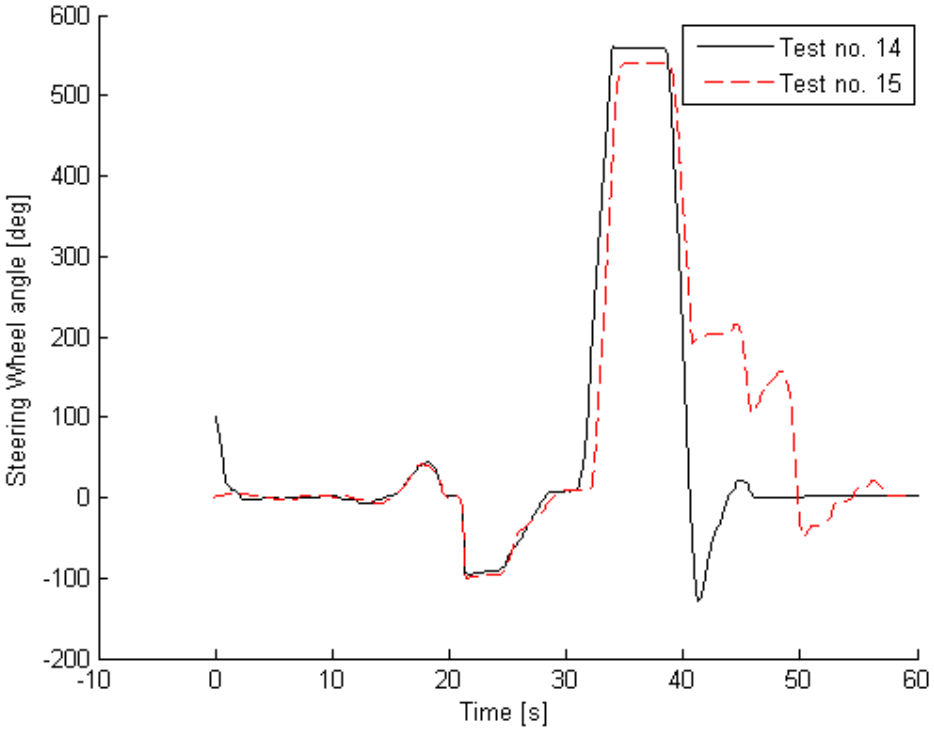

Figure C.11 SWA for test no. 14 and 15, Only SSRA control active.

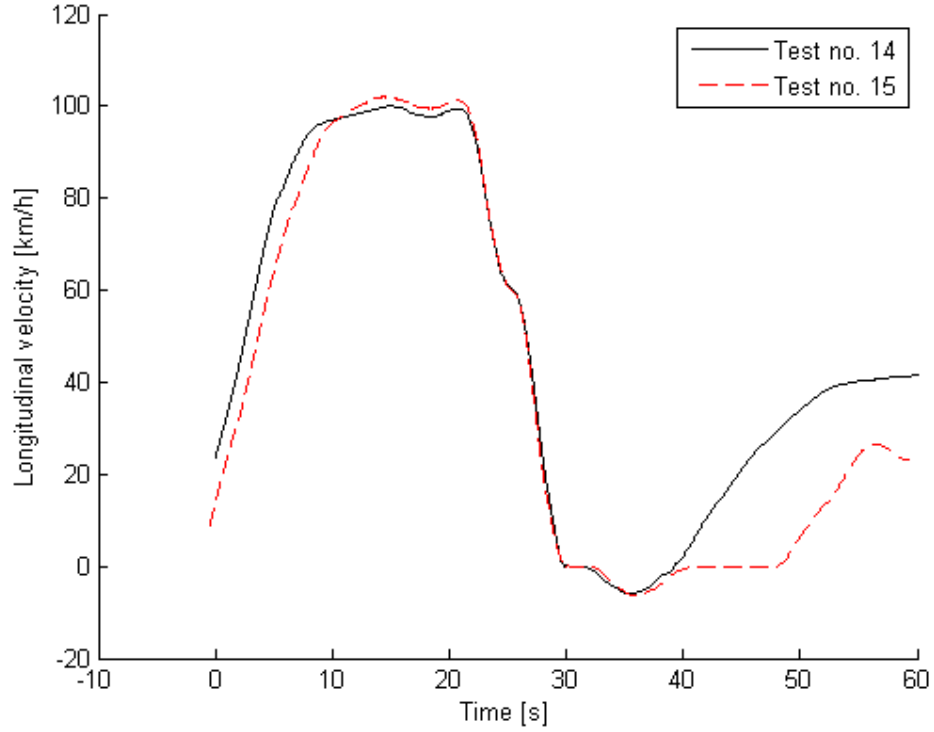

Figure C.12 Longitudinal speed for test no. 14 and 15, Only SSRA control active.

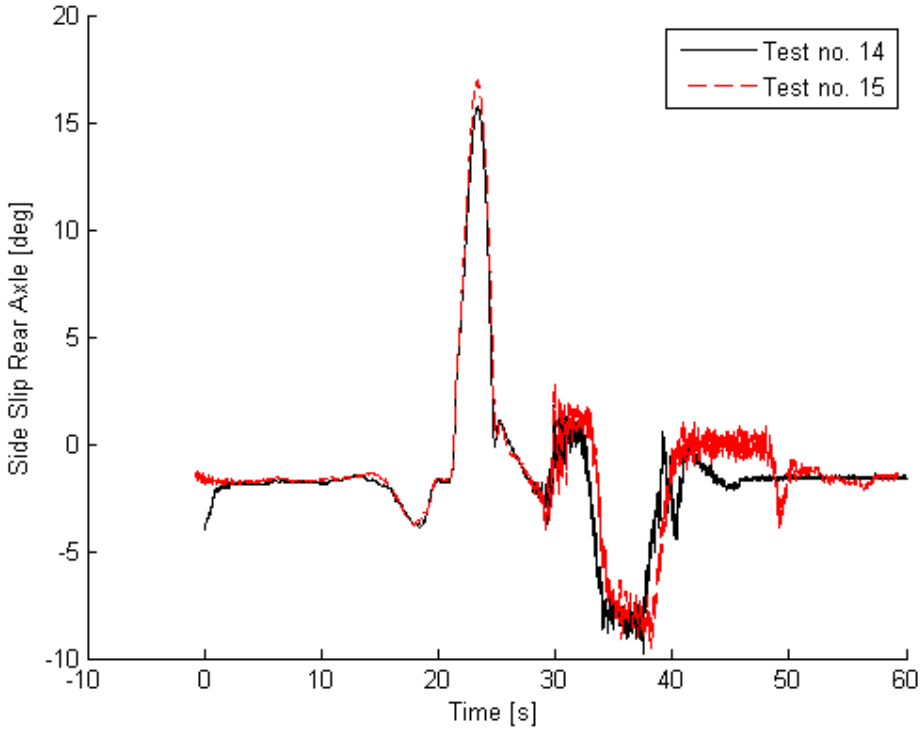

Figure C.13 Side slip angle at rear axle for test no. 14 and 15, Only SSRA control active.